

# Chapter 3

## Important Biological Events Occurring in Plants

### 3.1 Photosynthesis

*“Photosynthesis is an integrated system in which light harvesting, photo-induced charge separation, and catalysis combine to carry out two thermodynamically demanding processes, the oxidation of water and reduction of carbon dioxide.”*

- A part of the comment that appeared on the cover of the *Journal of Organic Chemistry*, **2006**, 71, issue no. 14, (July 7, 2006).

#### 3.1.1 Light Reaction: Formation of NADPH, ATP, and O<sub>2</sub>

“Photosynthesis is undoubtedly the most important single metabolic innovation in the history of life on the planet” [1]. It is looked upon as the mother of all biological events of life since essentially all free energy needed for biological systems originates from solar energy *via photosynthesis*, the most successful of all natural energy storage processes. Thus, all forms of life evolved to exploit oxygen for their well-being depend for their energy, directly or indirectly on this phenomenon, which truly belongs to an interdisciplinary field involving radiation physics, solid state physics, chemistry, enzymology, physiology, and ecology. The present discussion is mainly based on chemistry. Photosynthesis is a green plant process, the means of converting light into chemical energy, taking place into organelles called chloroplasts. In this process chlorophyll, the green coloring matter of plants utilizes the solar energy in converting CO<sub>2</sub> and H<sub>2</sub>O into carbohydrates, and oxygen and some water are evolved. Bacteria with bacteriochlorophyll can also achieve photosynthesis—bacteria do not evolve oxygen like green plants [2]. Since oxygen is a by-product of the green plant photosynthesis, the latter is sometimes called *oxygenic photosynthesis*, and it is the major source of oxygen in the atmosphere. The chemistry of the green plant or green algae photosynthesis will be discussed briefly. The plant photosynthesis utilizes the solar light. The bacterial photosynthesis utilizes the light in the infrared region. However, photons of far-infrared region

have too low energies to be utilized for any photochemical reaction. The splitting regions (approximately) of white sunlight, as seen after diffraction through prism or in rainbows (VIBGYOR), are shown in Fig. 3.1.

When white sunlight falls on **chlorophyll**, it absorbs light waves of all the wave lengths except at the region  $\sim 480\text{--}550\text{ nm}$ ; the region is attributed to green color of the VIBGYOR. Because of the nonabsorption and reflection of light of the green region, chlorophyll is green in color and hence the leaves are green. Richard Willstätter (1872–1942) (Appendix A, A30) won the 1915 Nobel Prize for elaborating the structure of chlorophyll. There are two major types of chlorophyll: chlorophyll-*a* (**Chl-a**) and chlorophyll-*b* (**Chl-b**) having the same structural scaffold, differing only in the ring B in having a  $\text{--CHO}$  group in **Chl-b** in place of a  $\text{CH}_3$  group in **Chl-a** (Fig. 3.2). This small change in the substituent causes a difference in energy absorption. The basic structure is named porphyrin possessing a tetrapyrrole skeleton, which contains an 18-membered ring with nine conjugated double bonds. The basic skeleton is thus aromatic and has its two canonical (resonance) forms contributing equally to their resonance hybrid. In Fig. 3.2, one canonical form is shown. However, like aromatic compounds either canonical form is used in the literature to represent the basic skeleton of the compounds shown in Fig. 3.2.  $\text{Mg}^{2+}$  is present at the center and is covalently bonded with two N atoms, and coordinately bonded to the other two N atoms of the porphyrin. **Chl-a** and **Chl-b**, thus called

Visible light (400-700 nm)

Color	Violet	Blue	Green	Yellow	Orange	Red	
$\lambda$ in nm	400	450	500	550	600	650	700

**Fig. 3.1** The electromagnetic radiation in the visible spectrum

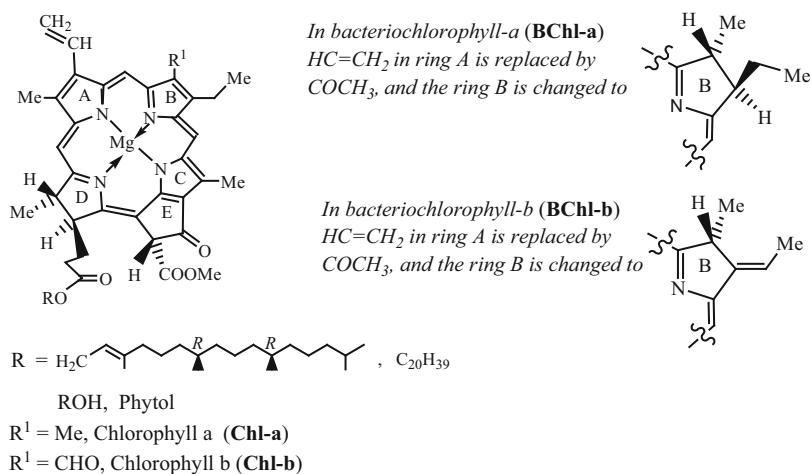


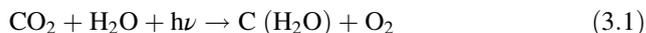
**Fig. 3.2** Stereostructures of **Chl-a**, **Chl-b**, **BChl-a** and **BChl-b**

magnesium porphyrins, are present in plants in the ratio 3:1. This ratio as well as their structures has remained the same during evolution, a very amazing feat of Nature. **Chl-a** does not absorb light in a wide range of the visible spectrum. This nonabsorbing region is known as the “green window”. The first absorption maxima of **Chl-b** and **Chl-a** are around 460 nm and 430 nm, respectively, and their second maxima are around 650 nm and 700 nm, respectively. **Chl-b** can transfer light energy very efficiently to **Chl-a**. Thus, the absorption gap of **Chl-a** green window is narrowed by the light absorption of **Chl-b**. Hence, the latter increases the efficiency of plants for utilizing sunlight energy.

The antenna protein containing many chromophores absorbs light. **Chl-a** is the central pigment of the plant photosynthesis. The trapped electromagnetic radiation of the sun causes the flow of energy within the photochemical apparatus containing specialized reaction centers, allowing the trapped energy to participate in a series of biochemical reactions. Because of the presence of a number of conjugated double bonds in the chlorophyll skeleton, much less amount of energy (photon of red light) is required to cause excitation of electrons to the lower energy first singlet state (half-life  $4 \times 10^{-9}$  s). The second singlet state requires higher energy (photon of blue light) and is of short half-life ( $10^{-12}$  s) to effect chemical reactions. Excited chlorophyll as such directly cannot transfer the energy to the right location. It initiates electron-transfer chain through electron acceptors like *quinones*, *cytochromes*, etc. resulting in a charge separation. In effect, the first singlet state splits water molecule into H and OH radicals. The OH radicals yield some oxygen and some water, while H reduces the oxidized coenzyme  $\text{NADP}^{\oplus}$  to **NADPH** (catalyzed by **ferredoxin NADP<sup>⊕</sup> reductase**, a **flavoprotein** with an **FAD** prosthetic group). The excess energy is stored as an energy-rich **ATP**, acting as a temporary source of energy. Its terminal  $\gamma$ -phosphoanhydride bond is hydrolyzed to yield **ADP** with the release of energy to be used in the biochemical processes, which are especially energetically unfavorable. ATP is rebuilt from ADP and Pi with the adequate input of energy. ATP is known as ‘energy currency’ in the cell. This forms the part of *light reaction* (Fig. 3.3).

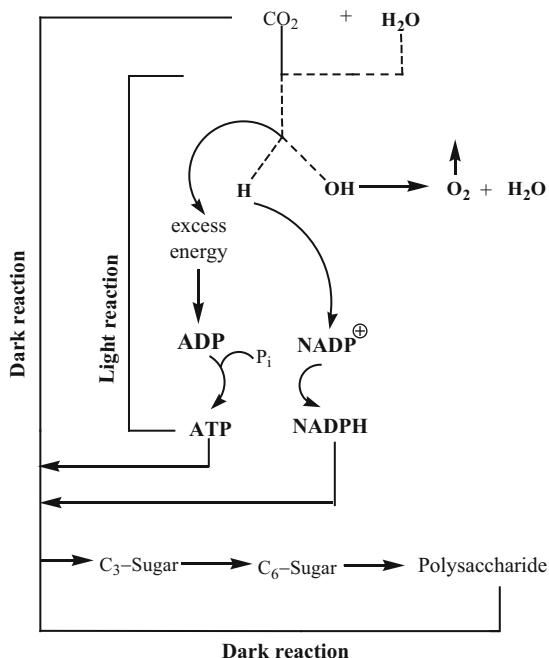
The reduced form of the coenzyme NADPH, a two electron donor, thus formed, reduces  $\text{CO}_2$  to 3-phosphoglycerate. Inorganic carbon is converted into the first organic molecule of the **carbon cycle (Calvin cycle)** to be discussed in the sequel.

The overall green plant photosynthesis reaction is represented by the century-old oversimplified basic expression (3.1) in which we find two thermodynamically demanding processes, oxidation of water and reduction of  $\text{CO}_2$  in the combined form.



Priestley in 1770s first showed by performing the following experiment that oxygen is liberated during photosynthesis. He put a mouse under each of two bell jars, one of which contained a plant while the other none. He found that the mouse in the bell jar containing the plant lived much longer than the other mouse. From this observation “. . . he correctly concluded that the plant, through interaction with

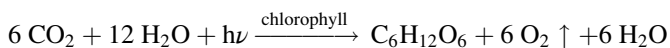
**Fig. 3.3** A simplified representation of photosynthesis in green plants



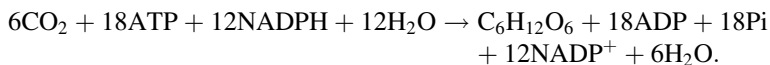
light, was modifying the air by producing a new substance. He set out to prove what this substance was and thereby discovered oxygen” [2]—a gas so convivial to our very existence. Melvin Calvin (NL, 1961) observed that plants/green algae upon irradiation with light in presence of  $^{14}\text{CO}_2$  produced labeled 3-phosphoglycerate, and he concluded that this  $\text{C}_3$ -sugar was the intermediate in the fixation of  $\text{CO}_2$  to saccharides. The unique enzymatic machinery present in the chloroplasts of green plants catalyzes the conversion of  $\text{CO}_2$  into simple organic compounds. This process is called *CO<sub>2</sub> fixation* or *carbon fixation*. The reactions involved make up a cyclic pathway constantly regenerating the key intermediates. The pathway was elucidated by Melvin Calvin in early 1950s and is often called the **Calvin cycle**. These simple products of photosynthesis are converted in plants into complex biomolecules like sugars, polysaccharides, and their metabolites.

Formation of NADPH and ATP takes place by the action of light and is called *light reaction*. In the *dark reaction*, the NADPH and ATP drive the reduction of  $\text{CO}_2$  to more useful organic compounds. A very simplified representation of photosynthesis is shown in Fig. 3.3.

To make a glucose molecule, six molecules of  $\text{CO}_2$  are needed as shown in the following equation:



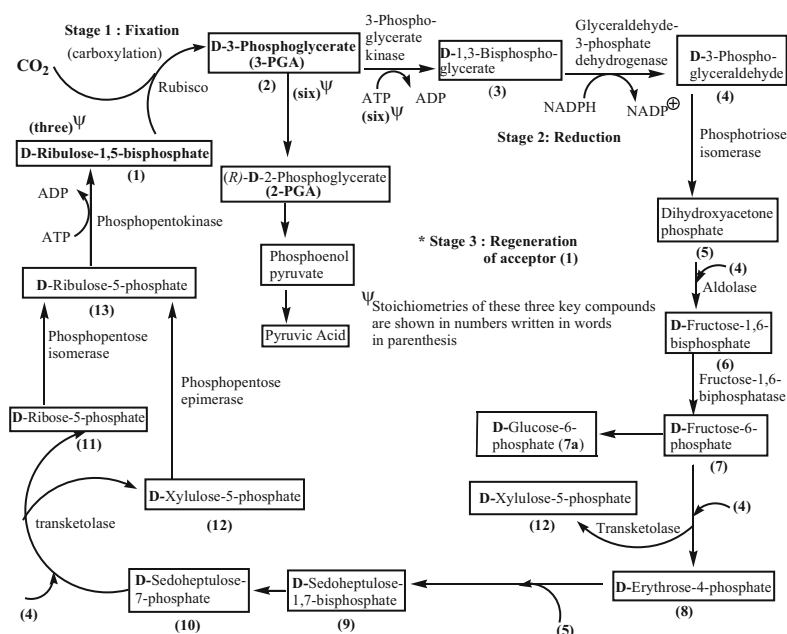
and the overall balanced equation for Calvin cycle may be represented as:



Interestingly, water appears on both sides of the equation. It is due to the fact that OH obtained from H<sub>2</sub>O gives oxygen as well as some water molecules.

### 3.1.2 Dark Reaction (Calvin Cycle): Formation of 3-, 4-, 5-, 6-, and 7-Carbon Sugars

Detailed studies by Melvin Calvin (NL 1961) and his collaborators revealed that photosynthetic CO<sub>2</sub> fixation proceeds by a cyclic process which has been named **Calvin Cycle** (Fig. 3.4). Since reduction occurs and pentoses are formed in the cycle, the latter is also termed as **reductive pentose phosphate (RPP) pathway**. The Calvin cycle consists of *three stages* (Fig. 3.4) to be explained in succession.



\* Stage 3 Regeneration of acceptor (1) from (4) via (5), (6), (7), (8) and so on, as shown.

(For mechanisms of all conversions see Figures 3.5 to 3.10)

**D,L-Nomenclature:** When the Fischer projection formula of the molecule is written placing (i) the more oxidized end of the chain at the top, and (ii) the longest carbon chain vertically, the enantiomer with the OH group at the lowermost (highest numbered) chiral center [e.g., C2 in (2), (3) and (4), C3 in (8), C4 in (1) and (12), C5 in (6), (7) and (7a), and C6 in (9) and (10)] on the right-hand side is given **D-configuration** - the corresponding enantiomer of each sugar is designated **L**.

**Fig. 3.4** Calvin cycle or carbon cycle: Formation of 3-, 4-, 5-, 6- and 7-carbon sugars in three stages

**Stage 1: The Fixation of CO<sub>2</sub> by Carboxylation of a C<sub>5</sub> Sugar to Form D-3-Phosphoglycerate (2)** In the fixation of CO<sub>2</sub>, the C<sub>5</sub> sugar D-ribulose-1,5-bisphosphate (for D,L-nomenclature see Fig. 3.4 and Sect. 2.6.1) acts as the acceptor on which carboxylation takes place in presence of an enzyme ribulose-1,5-bisphosphate carboxylase-oxygenase, commonly known as **rubisco/Rubisco** [3], *the most abundant protein in plant, and for that matter on earth. With its 16 subunits, it is one of the largest enzymes in nature. It is a lazy enzyme and its catalytic rate is 3 s<sup>-1</sup> only, i.e., it fixes only three molecules of CO<sub>2</sub> per second and causes its rich concentration in chloroplast* [4]. During the process, an unstable C<sub>6</sub> compound is formed which suffers rapid hydrolysis to yield two molecules of D-3-phosphoglycerate. Incorporation of CO<sub>2</sub> into 3-phosphoglycerate has been verified through the use of <sup>14</sup>CO<sub>2</sub>. Rubisco needs bound divalent Mg<sup>+2</sup> for its activation. Prior to carboxylation, D-ribulose-1,5-bisphosphate undergoes enolization via a complex formation with the enzyme active site, and Mg<sup>+2</sup>. The enediol form couples with CO<sub>2</sub> when a new carbon-carbon bond is generated. The adduct being unstable undergoes hydrolysis to yield two molecules of D-3-phosphoglycerate (Fig. 3.5).

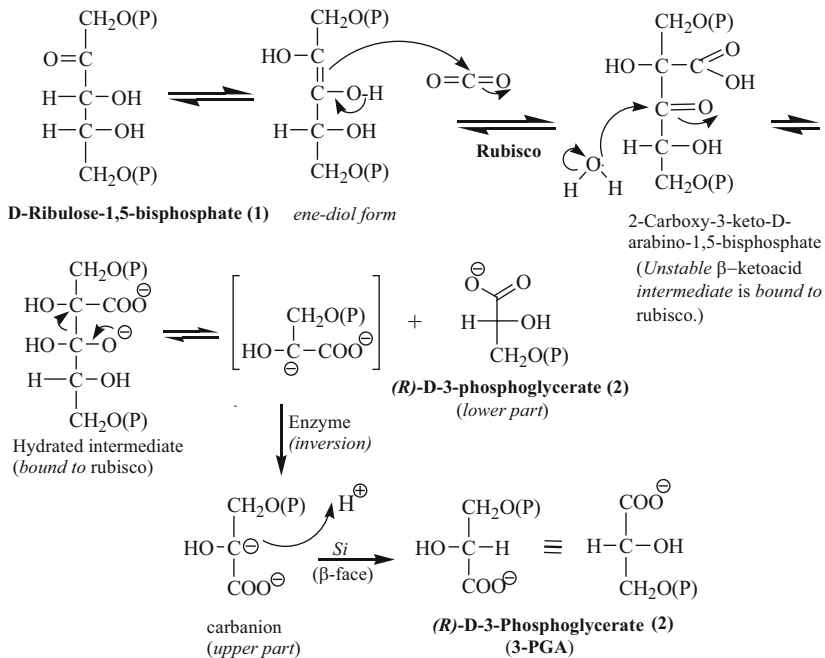


**Fig. 3.5** Stage 1 of the Calvin cycle: *Carboxylation*

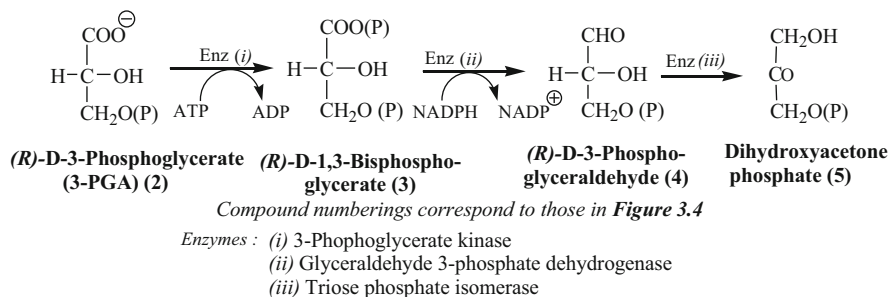


**Fig. 3.6** Stage 2 of the Calvin cycle: Formation of D-3-phosphoglyceraldehyde (4) and dihydroxyacetone phosphate (5)

**Stage 2: Formation of 3-Phosphoglyceraldehyde (4) and Dihydroxyacetone phosphate (5), the More Versatile Biosynthetic Precursors, by Reduction of 3-Phosphoglycerate (2)** Conversion of D-3-phosphoglycerate (2) to D-3-phosphoglyceraldehyde (4) takes place in two steps (Fig. 3.6). In the first step, 3-phosphoglycerate kinase catalyzes the transfer of phosphate from ATP to D-3-phosphoglycerate (2), yielding D-1,3-bisphosphoglycerate (3). In the second step, (3) is reduced by NADPH, being catalyzed by glyceraldehydes-3-phosphate dehydrogenase to form D-3-phosphoglyceraldehyde (4), which isomerizes to (5) in presence of triose phosphate isomerase.

**Stage 3: The Regeneration of the CO<sub>2</sub> Acceptor D-ribulose-1,5-bisphosphate (1)** The third stage of CO<sub>2</sub> fixation involves the remaining set of reactions of the Calvin cycle. The products of stage 2, viz., the triose phosphates (4) and (5) pass through a series of successive transformations to six-, four-, five-, and seven-carbon sugars, eventually leading to the regeneration of the starting material, D-ribulose-1,5-bisphosphate (1) in presence of a specific enzyme in each stereospecific step as shown in Figs. 3.7–3.9. Thus, a continuous flow of CO<sub>2</sub> into carbohydrates is maintained in the Calvin cycle. The H<sub>S</sub> of (5) attacks on the *Si* (or  $\alpha$ -) face of the carbonyl group of (4), being catalyzed by aldolase, to produce (6). In the next step, the transfer of CH<sub>2</sub>OH–CO– of (7) to the *Re* face of –CHO of (4) is effected by the transketolase enzyme whose prosthetic group, thiamine pyrophosphate (TPP), acts as the carrier. *Regeneration of D-ribulose-1,5-bisphosphate (1) and its formation from (4) and (5) via (6) to (13) in succession* are outlined and explained stepwise in Fig. 3.9.

The mechanism of the catalytic function of TPP is shown in Fig. 3.8.

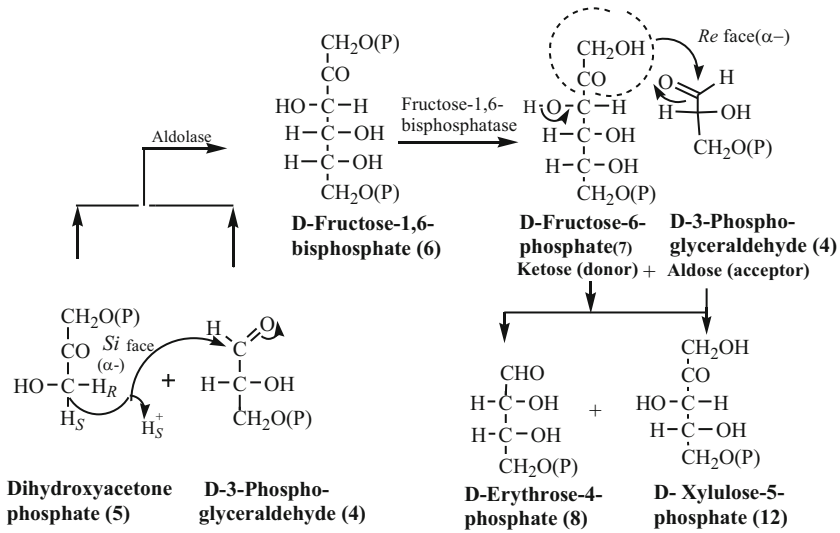


**Fig. 3.7** Stage 3 of the Calvin cycle (1st part): Formation of D-erythrose-4-phosphate (8) and D-xylulose-5-phosphate (12)

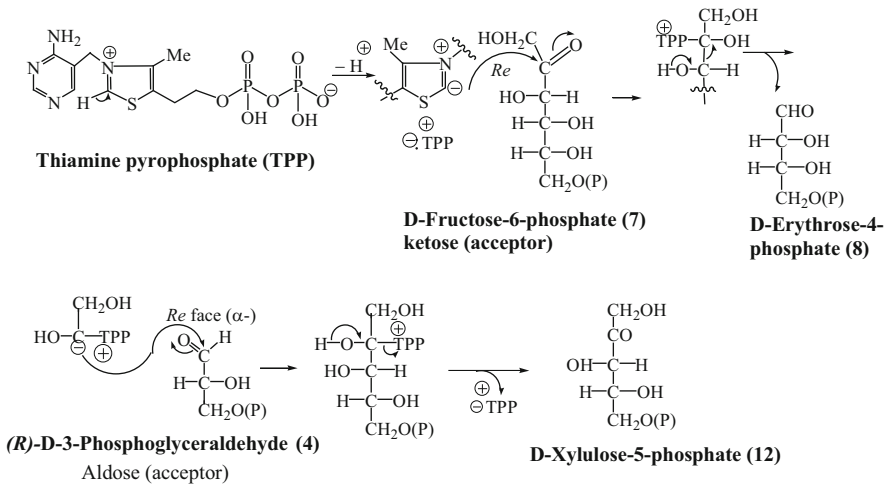
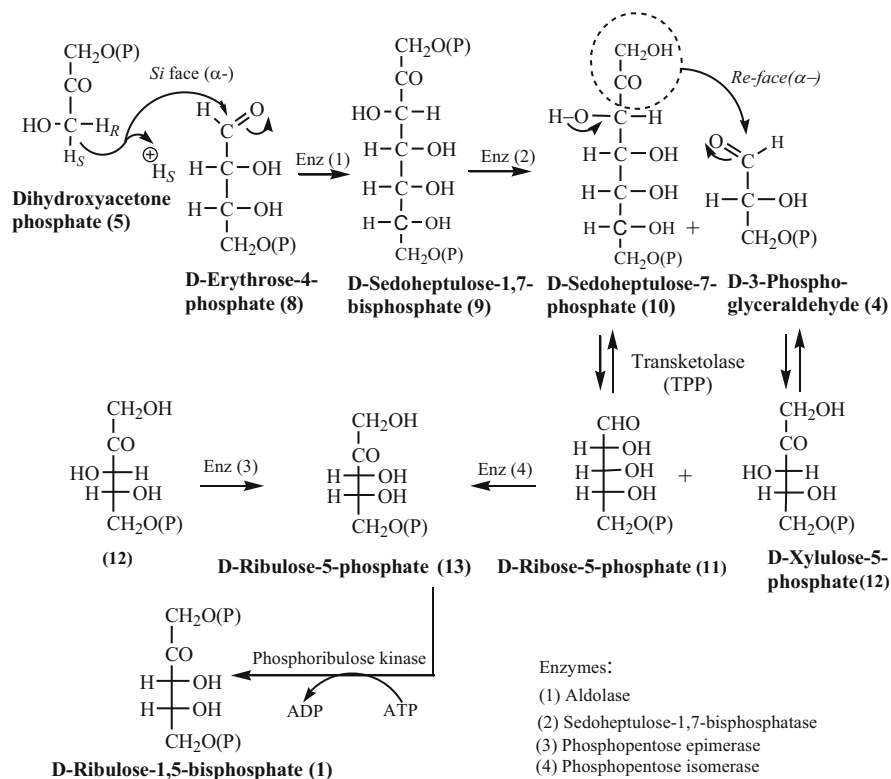


**Fig. 3.8** Function of TPP in the conversion of (7) to (8) and (12)

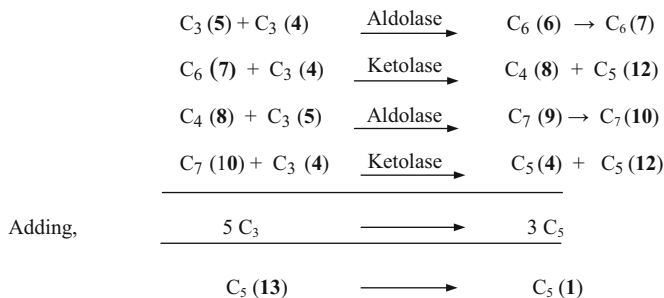


Compound numberings correspond to those in **Figure 3.4**

**Fig. 3.9** Stage 3 of the Calvin cycle (remaining part): Regeneration of D-ribulose-1,5-bisphosphate (1)

### 3.1.2.1 Some Comments and Implications Regarding Calvin Cycle Molecules

(i) The reactions can be summarized as follows:



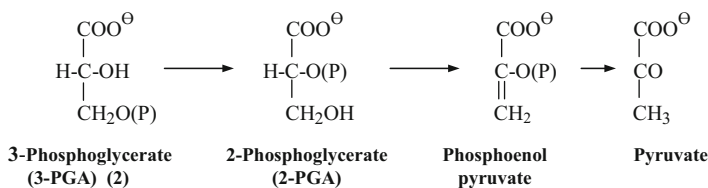


**Fig. 3.10** Stepwise conversion of 3-PGA to pyruvate

- (ii) Each of these C<sub>3</sub>, C<sub>4</sub>, C<sub>5</sub>, and C<sub>6</sub> molecules plays an important role in the biosynthesis of natural products.
- (iii) (*R*)-D-3-Phosphoglyceraldehyde, (**4**), generated in the 2nd stage of the Calvin cycle, serves as the mother molecule for the other sugars (4-, 5-, 6-, and 7-carbon sugars) including the CO<sub>2</sub> acceptor molecule D-ribulose-1,5-bisphosphate (**1**), preserving the stereochemical integrity of the chiral center of (**4**), which becomes the lowermost chiral carbon. Hence, according to IUPAC nomenclature, all the sugars are named D-sugars (Chap. 2). Apparently, in the plant cells, no enzyme is available which can epimerize the designated chiral carbon of the sugars producing an L-diastereomer, although epimerization at other centers in presence of specific epimerases is known.
- (iv) Most of the D-glyceraldehyde-3-phosphate (**4**) is recycled to D-ribulose-1,5-bisphosphate (**1**). The remaining (**4**) may be used immediately as a source of energy, converted to sucrose for transport *via* its precursor D-fructose-6-phosphate (**7**), or stored as *starch* for future use. The part of dihydroxyacetone phosphate (**5**), which is not used in Calvin cycle, leaves the chloroplast and can be degraded *via* glycolysis to provide energy.
- (v) 3-Phosphoglycerate (**2**) (3PGA) gives rise to pyruvate at the primary metabolic level as shown in Fig. 3.10.
- (vi) 3PGA may also be formed by the breakdown of D-glucose *via* D-fructose 1,6-diphosphate (**6**)
- (vii) Pyruvic acid is a very important key compound. It forms acetyl coenzyme A; the latter enters into the formation of fatty acids, polyketides (Chap. 14), and aromatic compounds and also terpenoids and steroids *via* mevalonic acid pathway (Chaps. 5, 5, and 11).

### 3.1.3 C<sub>4</sub>-Plant Photosynthesis, C<sub>3</sub>- and C<sub>4</sub>-Plants

As discussed above, a C<sub>3</sub>-acid, phosphoglyceric acid (PGA) is the primary fixation product in the *Calvin cycle* of the carbon fixation process. PGA is formed mostly in the chloroplast present in the leaf *mesophyll* tissues involving *rubisco* having both carboxylase and oxygenase catalytic activities. Because of the latter activity of the enzyme which is less suppressed by comparatively low CO<sub>2</sub> intake from air (CO<sub>2</sub> concentration being much less than that of O<sub>2</sub>), a considerable part of fixed carbon

is oxidized and lost as  $\text{CO}_2$ —a phenomenon known as *photorespiration* resulting into a significant loss of energy. Thus this process is inefficient.

Subsequent to the discovery of Calvin cycle, Hugo Kortschak obtained an unexpected result while studying the photosynthesis with  $^{14}\text{CO}_2$  in sugarcane (at the Sugarcane Research Institute, Hawaii), in which  $\text{C}_4$ -acids, viz., oxaloacetate and malate appeared as the primary fixation products. Kortschak did not publish this observation in any journal. Ten years later, a Russian scientist Yuri Karpilov made a similar observation in the maize plant. This observation challenged the universality of the Calvin cycle. However, Hatch and Slack [5, 6] solved this riddle. It was then generalized that in some plants, prior to the Calvin cycle,  $\text{CO}_2$  is prefixed as some  $\text{C}_4$  acids like *oxaloacetate* and *malate*, as the primary fixation products. It was suggested that such fixation takes place in leaf cells with Kranz (meaning garland/wreath)-type anatomy (a few exceptions) having a wreath type arrangement of cells, with the *inner bundle sheath cells* being surrounded by *mesophyll tissue cells*.

Initial fixation to D-*malate* takes place in the outer *mesophyll* tissues, which lacks rubisco. Atmospheric  $\text{CO}_2$  is converted to  $\text{HCO}_3^-$  catalyzed by *carbonic anhydrase*, which is absent in  $\text{C}_3$ -plants. The bicarbonate anion reacts with *phosphoenol pyruvate* (PEP), being catalyzed by PEP carboxylase to form oxaloacetate, which is then enzymatically reduced to malate (Fig. 3.11). The metabolic product malate is transferred to *bundle sheath* cell zone through a mechanism involving *plasmodesmata* (intercellular connections), since the bundle sheath cell wall is impermeable to the fixation products. D-Malate forms pyruvate and releases  $\text{CO}_2$  to *rubisco* as its substrate to enter into Calvin cycle (Fig. 3.11). The pyruvate moves to mesophyll tissue cells, gets phosphorylated to form PEP, which is reused in the oxaloacetate formation, and the cycle is repeated.

In some plants (e.g., millet and forage plants) glutamate aspartate transaminase concentration being higher, oxaloacetate is transaminated to aspartate (in presence of glutamate), which moves to bundle sheath cells. There it is reconverted to oxaloacetate that in turn enzymatically releases  $\text{CO}_2$  and forms PEP (Fig. 3.11). Initially, the concentration of oxaloacetate is not sufficiently high to allow its participation in the metabolic flux to diffuse from mesophyll tissue cells to bundle sheath cells. Hence, it moves via malate or aspartate. This pathway is known as Hatch and Slack pathway.

Thus, two major pathways,  $\text{C}_3$ -acid pathway (Calvin cycle and RPP cycle) and  $\text{C}_4$ -dicarboxylic acid pathway (Hatch and Slack pathway and  $\text{C}_4$ -pathway), are followed in photosynthesis, and according to the primary fixation products the plants are classified as ***C<sub>3</sub>-plants*** (most plant species belong to this class) and ***C<sub>4</sub>-plants*** (mostly pasture plants, crops, forage plants, wild weeds, desert plants, etc.). In  $\text{C}_3$ -plants *rubisco* is the primary enzyme while in  $\text{C}_4$ -plants phosphoenol pyruvate carboxylase (*PEP carboxylase*) is the key enzyme.

In  $\text{C}_4$ -plants, there is no rubisco in the mesophyll tissue cells, but some rubisco is present exclusively in bundle sheath cells.  $\text{C}_4$ -Plants need less rubisco, less nitrogen, and also less water for growth. So in warm weather,  $\text{C}_4$ -plants grow advantageously. However,  $\text{C}_4$ -plants are affected by chilly weather.

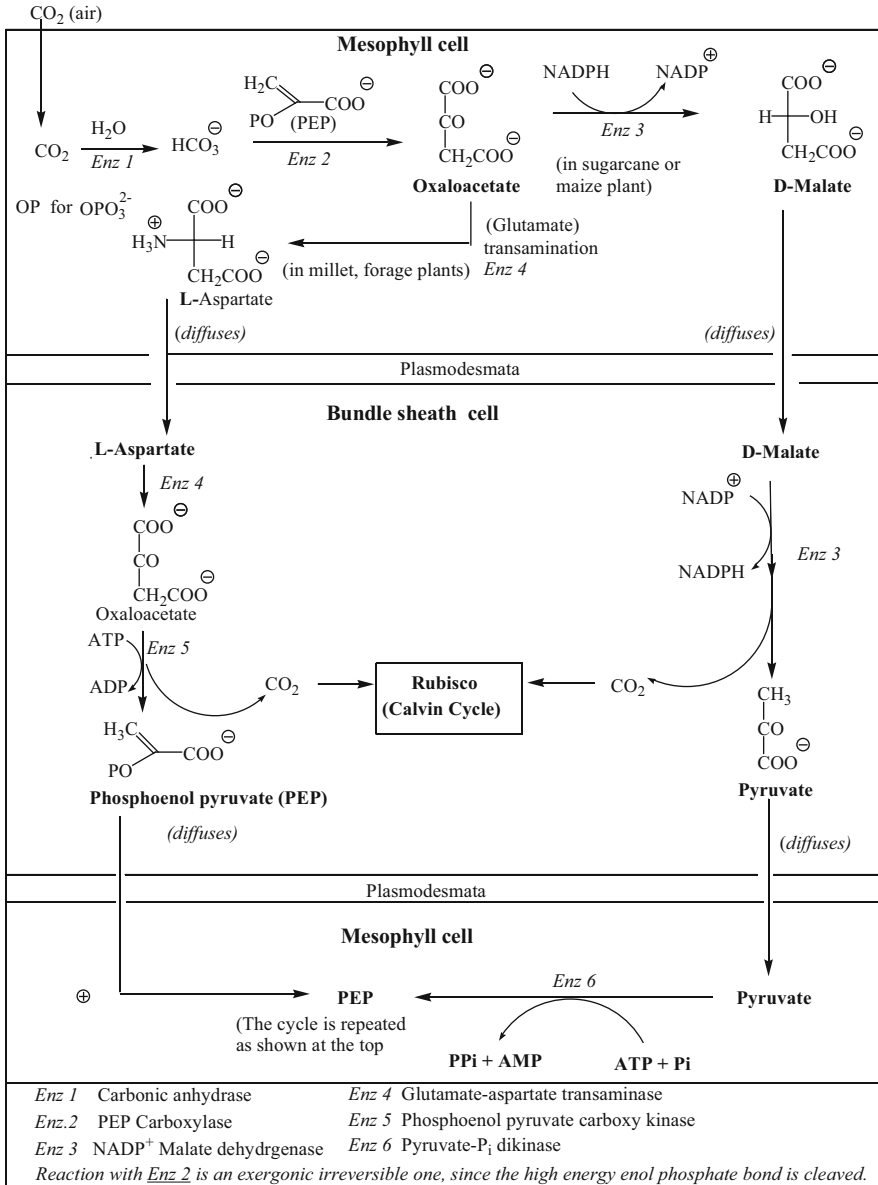


Fig. 3.11 C4- Plant photosynthetic cycle

### 3.1.3.1 Identification of $\text{C}_3$ and $\text{C}_4$ Metabolism Products by Mass Spectrometry

The natural isotopes of carbon are  $^{12}\text{C}$  (98.89 %) and  $^{13}\text{C}$  (1.11 %). Because of the kinetic isotope effect rubisco reacts faster with  $^{12}\text{CO}_2$  than with  $^{13}\text{CO}_2$  in  $\text{C}_3$  plants, resulting in the lowering of  $^{13}\text{C}/^{12}\text{C}$  ratio in the products of  $\text{C}_3$  photosynthesis than this ratio in the atmospheric  $\text{CO}_2$ . In  $\text{C}_4$ -metabolism, the enzymatically prefixed  $\text{CO}_2$  with less kinetic isotope effect reacts with rubisco in bundle sheath cells and thus such lowering of the  $^{13}\text{C}/^{12}\text{C}$  isotope ratio in the photosynthesis products is less. Hence by studying the  $^{13}\text{C}/^{12}\text{C}$  ratio in the product mass spectrometrically, it is possible to predict the metabolism pathway followed to form the product. For example, sugar obtained from two different sources, e.g., sugar beet ( $\text{C}_3$ -plant) as well as sugarcane ( $\text{C}_4$ -plant) can be related to its source by its isotope ratio analysis. In  $\text{C}_4$  Pathway, photorespiration is almost absent due to high concentration of  $\text{CO}_2$  released by the prefixed  $\text{C}_4$  products, and the suppression of the enzymatic oxygenase activity of rubisco due to absence of  $\text{O}_2$ .

### 3.1.3.2 Crassulacean Acid Metabolism (CAM)

The plants like all cacti and many desert plants growing in arid zones, the succulent ornamental plant *Kalanchoe* and plants growing in tropical rain forests, including half of the orchids manage the extreme shortage of water by keeping their leaf stomata closed during daytime to avoid loss of water, and reduce the area of their leaves. They open their leaf stomata in the night to allow the entry of  $\text{CO}_2$  and to mask evaporation.  $\text{CO}_2$  is prefixed as  $\text{C}_4$ -acids and stored in the vacuole until next morning when they are degraded to release  $\text{CO}_2$  to rubisco in the chloroplasts; the pyruvate formed is subsequently phosphorylated by pyruvate phosphate kinase. The major difference in this case is the time lag between  $\text{CO}_2$  fixation (storage) and its release. The mechanism has been first studied in Crassulaceae plants, and  $\text{CO}_2$  is stored as an acid and hence the name crassulacean acid metabolism (**CAM**). Pineapples and the agave sisal, yielding natural fibers are important **CAM plants**.

## 3.2 Biological Oxidation: Reduction ( $\text{NADPH} = \text{NADP}^+$ )

As mentioned earlier (Chap. 1), there are enzymes which are coenzyme or cofactor dependent in their functions. Enzyme promoted oxidation–reduction in the biological systems uses several coenzymes. The function of one such coenzyme, nicotinamide adenine dinucleotide phosphate [in the reduced ( $\text{NADPH}$ ) (**15**) and oxidized ( $\text{NADP}^\oplus$ ) (**14**) forms] (Fig. 3.12) will be discussed briefly. They act in a large number of oxidation–reduction reactions. Sometimes,  $\text{NADPH}$  has been compared to the laboratory reagent  $\text{NaBH}_4$  by describing it as Nature's  $\text{NaBH}_4$ . However, the

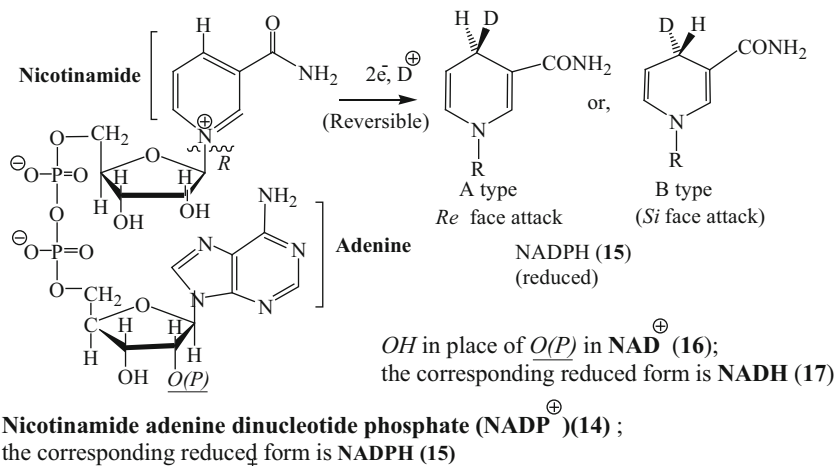


**Fig. 3.12** Structures of  $\text{NADP}^{\oplus}$ ,  $\text{NADPH}$ ,  $\text{NAD}^{\oplus}$  and  $\text{NADH}$

latter being achiral and incapable of being reversed like a redox system, such a comparison is hardly reasonable. However, Hantzsch 1,4-dihydropyridine has been widely used as a biomimetic reducing agent (cf.  $\text{NADPH}$ ) (Chap. 13).

The coenzyme is tightly bound to the enzyme by multiple noncovalent interactions in a dissociable fashion. Many oxidation–reduction involving enzymes carry out electron transfer through the agency of  $\text{NADPH}/\text{NADP}^{\oplus}$ . The nicotinamide part of the coenzyme is responsible for the biological oxidation–reduction reaction and constitutes an example of a biological redox system; its  $\text{CONH}_2$  part ensures its redox potential; and the R part controls the binding of the coenzyme to the enzyme. The word ‘**redox**’ is the abbreviated form of ‘**reduction–oxidation**’.

The term oxidation finds its genesis in terms of addition of oxygen (or removal of hydrogen) and reduction consists of removal of oxygen (or addition of hydrogen). They can better be explained in terms of electron gain (reduction) and electron loss (oxidation) during the process.

The nicotinamide end of the coenzyme participates in the oxidation–reduction of a substrate molecule by way of a hydride removal and acceptance, at the same time the concerned moiety of the coenzyme undergoing reduction and oxidation (Fig. 3.13). Enzymatic reactions are stereospecific; of the two diastereotopic hydrogen atoms ( $\text{H}_R = \text{H}_A$  and  $\text{H}_S = \text{H}_B$ , see Chap. 2) of  $\text{NADPH}$  (C4 being prochiral),  $\text{H}_R$  with its bonded electron pair (hydride) is transferred to the substrate to effect its reduction,  $\text{NADPH}$  itself being converted to its oxidized form  $\text{NADP}^{\oplus}$ . In the reverse process, i.e., during oxidation of the substrate, the same hydrogen ( $\text{H}_A$ ) with its bonded electron pair is delivered to the *Re* face of  $\text{NADP}^{\oplus}$  to convert it to  $\text{NADPH}$ , and  $\text{H}_A$  now becomes  $\text{H}_R$ . Some enzymes use the *pro-S* (or  $\text{H}_S$ ) in a similar fashion.

The stereospecificity of several oxidation–reduction processes caused by biological redox system with respect to the substrate and the coenzyme has been

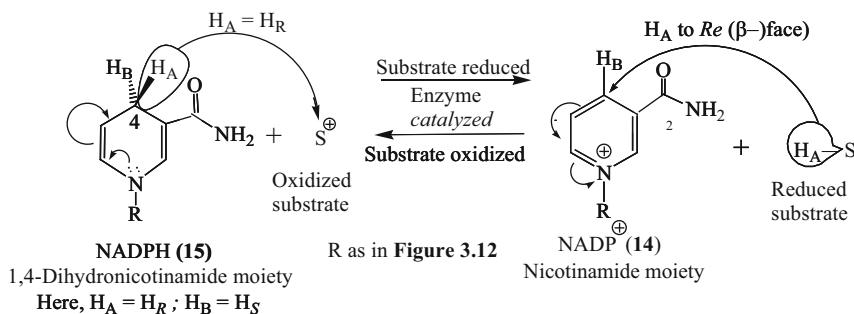


**Fig. 3.13** Stereospecific delivery and acceptance of hydride by NADPH and NADP + respectively.

proved by labeling the key hydrogen by deuterium/tritium. The stereochemical information is delivered at the site of attack depending on the *diastereofacial differentiation*, as illustrated in Fig. 3.13.

Incubation of the alcohol dehydrogenase with  $\text{CH}_3\text{CD}_2\text{OH}$  in presence of the cofactor  $\text{NAD}^+$  (**16**) generates the reduced cofactor (**17a**) (Fig. 3.14). The latter is reoxidized by  $\text{CH}_3\text{CHO}$  to  $\text{NAD}^+$  (**16**), the former being reduced to *1R*-deuteroethanol, demonstrating that the D atom transferred to the cofactor at C4 at its *Re* face is stereospecifically removed in the reverse reaction to attack the *Re* face of  $\text{CH}_3\text{CHO}$ , forming the chiral *1R*-deuteroethanol. In the reverse reaction (*1R*)-deuteroethanol when incubated with  $\text{NAD}^+$  (**16**) in presence of the enzyme regenerates only *4R*- $^2\text{H}$ -NADH (**17a**) with complete transfer of D to its *Re* face. Evidently, the rigorous stereochemical control of enzyme catalyzed reactions is brought about by the precise positioning of the substrate and the coenzyme at the enzyme active site.

The interconversion  $\text{NAD}^+$  (**16**) = NADH (**17a**) and their phosphorylated analogs  $\text{NADP}^+ = \text{NADPH}$  can be monitored *in vitro* by UV spectroscopy. Both the oxidized forms show one absorption band around 260 nm, whereas reduction to NADH or NADPH produces a new broad absorption band with a maximum of 340 nm. Thus, the production of NADH or NADPH during an enzyme-catalyzed oxidation of a substrate can be conveniently followed by observing the appearance of the  $\lambda_{\text{max}}$  at 340 nm. We cite here another example of diastereospecific enzymatic reduction by NADH. It occurs during *souring of milk*.

*Glycolysis*, a part of *fermentation*, is a ten-step pathway converting one molecule of glucose to two molecules of pyruvate. A lactic acid bacterium uses a direct route to effect an enantiospecific reduction of pyruvate to *S*-L-lactate with NADH in presence of the enzyme lactate dehydrogenase (Fig. 3.15). Here, an electron pair from NADH attacks the *Re* (front) face of pyruvate. *Souring of milk* involves this endergonic reaction.

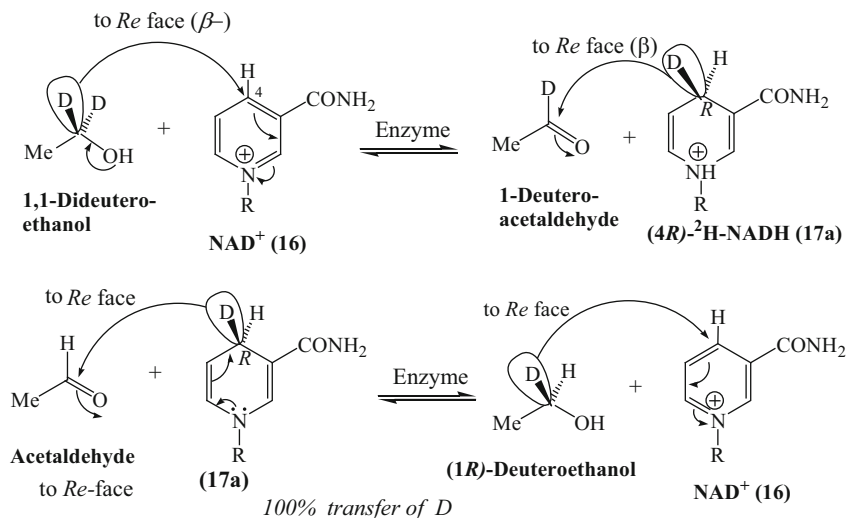


Fig. 3.14 Stereospecificity of alcohol dehydrogenase

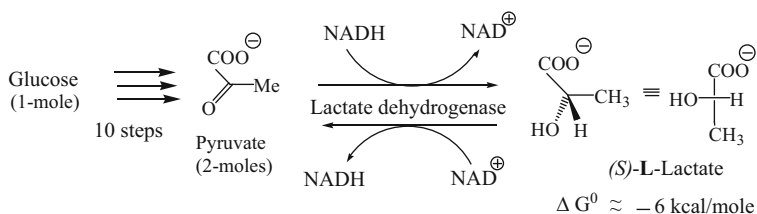
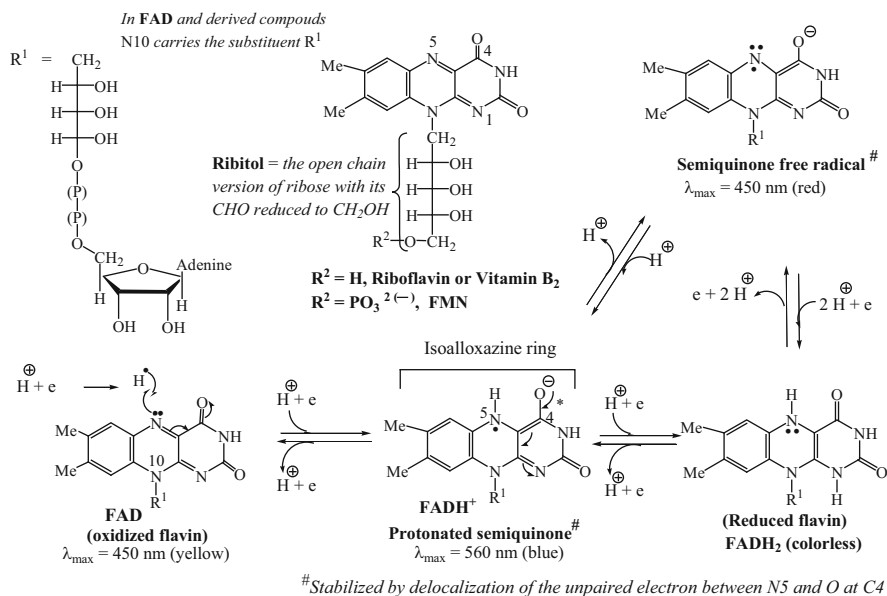


Fig. 3.15 Enantiospecific reduction of pyruvate to L-lactate (during souring of milk)

### 3.2.1 Flavin Coenzymes

Two coenzymes, flavin adenine dinucleotide (FAD) and flavin mononucleotide (FMN), are derived from vitamin B<sub>2</sub> or riboflavin. FMN is riboflavin phosphate (Fig. 3.16). Functionally both types are equivalent. Some enzymes use FAD while some others use FMN. Highly conjugated tricyclic isoalloxazine ring system, the functional part of both coenzymes, serves as a two-electron acceptor and is responsible for its strong redox character toward diverse classes of compounds. Molecules possessing such a ring system are called flavins. Flavin coenzymes are used by enzymes called flavoproteins (flavoenzymes). The latter bind FMN or FAD in most cases noncovalently but tightly so that the coenzymes can be reversibly dissociated. The flavins undergo two-electron oxidation and reduction reactions. They have a stable species, a semiquinone free radical produced by one-electron reduction that can be detected spectrophotometrically. The oxidized flavins are bright yellow;



**Fig. 3.16** Flavin coenzymes and the mechanism of their redox reactions

protonated semiquinone is blue, the semiquinone free radical is red, but the fully reduced flavins are colorless. The flavins have catalytic versatility more than nicotinamide coenzymes, since they can interact with two-electron or one-electron donor–acceptor pairs. Mechanism of stepwise reduction of FAD to  $\text{FADH}_2$  via  $\text{FADH}^+$  (protonated semiquinone) is shown in Fig. 3.16.

### 3.2.2 Combined Use of NADPH and FAD

There are cases when the substrate molecule is not directly reduced by NADPH (or NADH). Transfer of hydride from NADPH (or NADH) takes place indirectly. Two electrons are delivered from NADPH to a second enzyme cofactor, e.g., FAD in two steps to the N5 in the isoalloxazine ring, accompanied by accepting one proton from the medium in each step to form  $\text{FADH}_2$ . The latter delivers two electrons to the substrate to reduce it, itself being oxidized to FAD (Fig. 3.17).

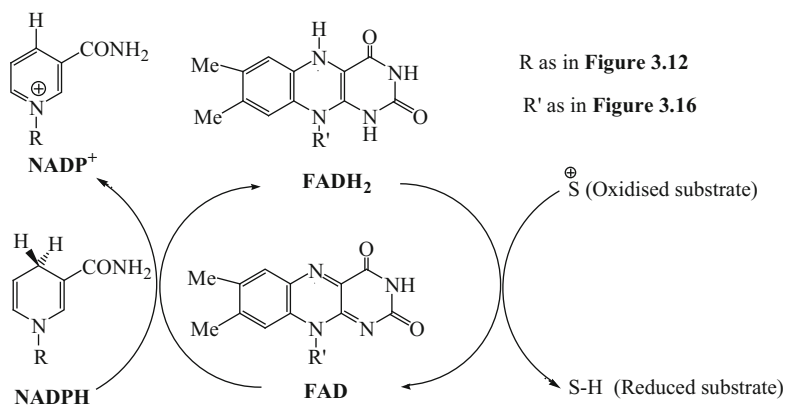


Fig. 3.17 Reduction by NADPH/FAD through FADH<sub>2</sub> in presence of enzyme

### 3.3 Phosphorylation (ATP→ADP) and Regeneration (ADP→ATP)

#### 3.3.1 Function of ATP: Its Conversion to ADP

Adenosine triphosphate (**18**) (Fig. 3.18), abbreviated as ATP, is one of the major cofactors in many metabolic biosynthetic pathways. It acts as the phosphate donor to the appropriate substrates and is biologically a potential source of metabolic energy. It is considered to be the key molecule for capturing and storing chemical energy. It moves through the cells providing energy for all processes of the cells [1]. It contains one ester and two anhydride phosphoryl groups ( $\beta$ - and  $\gamma$ -), and the 5'CH<sub>2</sub> group where nucleophilic attack could take place. Its  $\gamma$ -phosphate group is transferred to various acceptors to activate them for their subsequent participation in various biological events. In unusual cases, attack on C5' of the adenosyl part takes place, e.g., the formation of *S*-adenosyl methionine (SAM or AdoMet) (see Sect. 3.6).

*The function of ATP in various biochemical reactions* has been illustrated, whenever necessary (e.g., formation of mevalonic acid and  $\gamma,\gamma$ -dimethylallyl pyrophosphate, see Chap. 5). It has been observed that during pyrophosphorylation of alcoholic OH group (e.g., mevalonic acid to mevalonic acid pyrophosphate, Chap. 5, Fig. 5.3), two molecules of ATP are needed. Each ATP molecule donates its  $\gamma$ -phosphate group to the substrate and is converted to ADP. Presumably, the incapability of ATP for donating two phosphate groups in succession (ATP→ADP→AMP) is prevented by the spatial incompatibility of ADP to work as coenzyme with phosphorylating enzyme for such a reaction. The ATP can be hydrolyzed to adenosine diphosphate (ADP) (**19**) by shedding off the  $\gamma$ -phosphate.

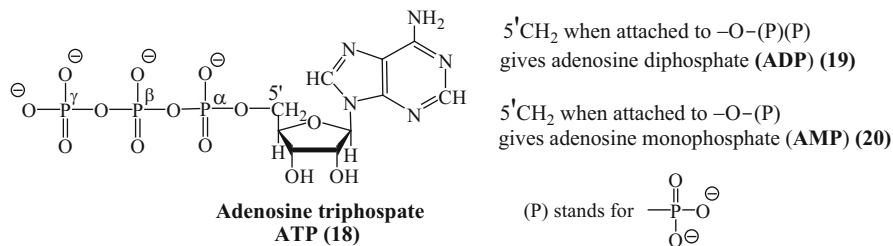


**Fig. 3.18** Structures of ATP(18), ADP(19) and AMP(20)



The negative standard free energy  $\Delta G^0$  is a measure of the ability of its phosphoryl group transfer potential. However, it has been shown that standard free energy of the hydrolysis of ATP depends on the water concentration. In the absence of water, the above reaction is directed towards ATP formation, and much energy is not needed. The reaction site of ATP formation in the enzyme can exclude water molecules and may proceed without the consumption of energy. Actually, energy requirement is necessary for certain conformational change in the catalytic sites of the enzyme and finally to release the ATP from the binding site.

### 3.3.2 Conversion of ADP to ATP

Adenosine diphosphate (ADP) can be reconverted to ATP by uniting with inorganic phosphate and with an adequate input of energy. In the leaf cells, during photosynthesis ADP is converted to ATP (photophosphorylation) (Fig. 3.3) by solar energy, and also in almost all cells by aerobic oxidation (oxidative phosphorylation) using chemical energy.

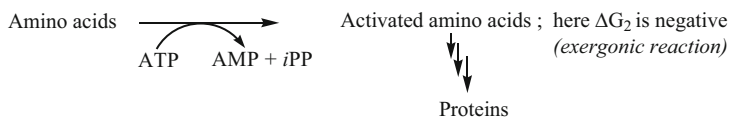
### 3.3.3 Formation of Proteins from Amino Acids

ATP favors thermodynamically unfavorable reactions like peptide bond formation. Calculations show that polymerization of amino acids to protein in the absence of ATP should be *endergonic*, i.e.,  $\Delta G$  becomes positive.



However, ATP activates the amino acid by cellular reaction involving ATP breakdown to adenosine monophosphate (20) (AMP), giving more negative  $\Delta G$

( $-45.6$  kJ/mol). The sum total free energy change for the formation of protein becomes negative. Since  $\Delta G_2 \ll \Delta G_1$  (the magnitude of the negative  $\Delta G_2$  being much more than the positive  $\Delta G_1$ ), the overall reaction becomes thermodynamically favorable.



### 3.3.4 Biosynthesis of Starch with the Help of ATP

Similarly in the biosynthesis of starch, polymerization of glucose takes place through the participation of ATP (Fig. 3.19). Different plants perceive a variety of environmental and endogenous influences, and as a consequence various chemical components including starch, differ in the composition. Amylose, one form of starch contains repetitive units of glucose united *via*  $\alpha$ -1,4- disaccharide linkage.  $\alpha$ -D-Glucose-1-phosphate reacts with ATP reversibly to give ADP-glucose. The pyrophosphate formed is hydrolyzed by the enzyme *pyrophosphatase* and in this way the formation of ADP-glucose becomes irreversible. The glucose activated by

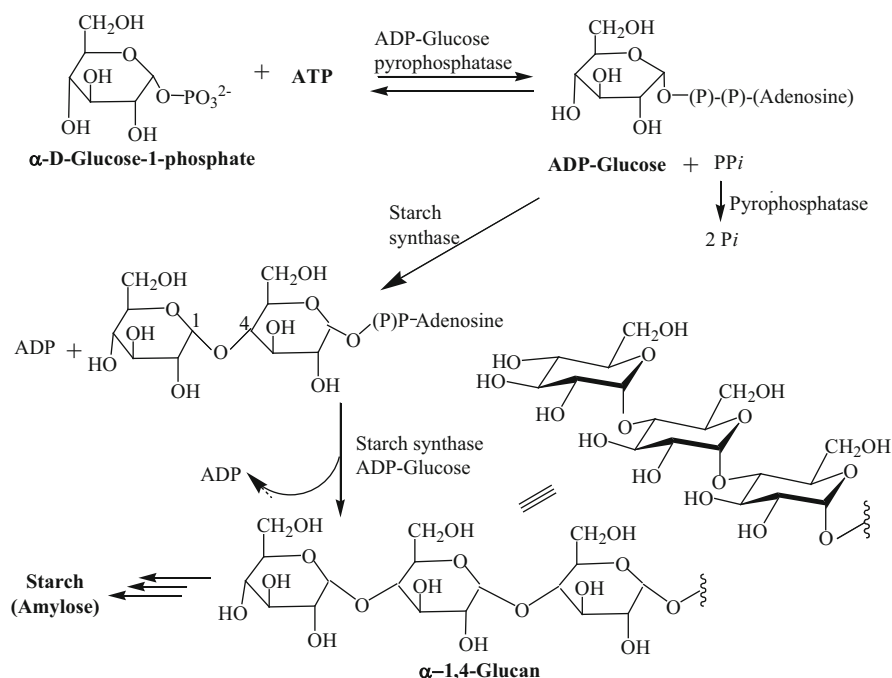


Fig. 3.19 Biosynthesis of starch (amylose) from  $\alpha$ -D-glucose

ADP is transferred by starch synthase from ADP-glucose to the OH group in the 4-position of the terminal glucose residue in the polysaccharide chain in the formative stage of starch. Similar deposition of glucose residue ( $\alpha$ -1,4-disaccharide linkage) continues, catalyzed by starch synthase to form starch.

### 3.4 Acetyl Coenzyme A

The discovery of the cofactor, acetyl coenzyme A (**21**) (Fig. 3.20), an essential biochemical reagent for many diverse biological reactions, led to a major advance in the field of biochemistry. Structurally, it has three units:  $\beta$ -mercaptoethylamine, pantothenate (vitamin B<sub>5</sub>), and 3'-phosphoadenosine-5'-diphosphate units, as shown in its structure (**21**).

Breslow provided evidence (IR, NMR) for the detection of stable thiazolium zwitterions of model thiazolium compounds by deuterium exchange studies in D<sub>2</sub>O [7]. He thus suggested a mechanism involving such a zwitterion for the thiamine pyrophosphate (TPP<sup>+</sup>) (Fig. 3.21) catalyzed *in vivo* biochemical reactions, e.g., decarboxylation of  $\alpha$ -keto acids like pyruvic acid and benzoyl formic acid.

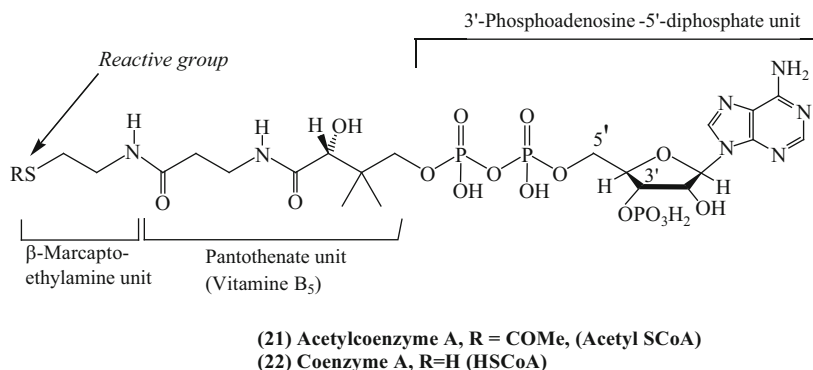


Fig. 3.20 Structures of acetyl coenzyme A and coenzyme A

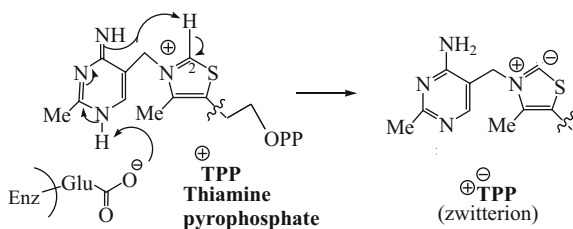


Fig. 3.21 Generation of TPP carbanion

Many other acids are also known to be activated as the corresponding acyl coenzyme A, e.g., malonyl coenzyme A, glutaryl coenzyme A, benzoyl coenzyme A, etc. The acyl coenzymes are responsible for many biological reactions.

### 3.4.1 Formation of Acetyl Coenzyme A from Pyruvic Acid

The stepwise mechanism of the formation of acetyl coenzyme A (**21**) by TPP<sup>+</sup> catalyzed decarboxylation of pyruvic acid is shown in two parts:

- (a) **Generation of TPP carbanion.** It has been shown from NMR and IR studies that the pyrimidine ring of TPP participates in the generation of the carbanion at C2 of the thiazole ring. It is initiated by the abstraction of the proton from the pyrimidine tautomer by the glutamate carboxyl group of the enzyme as shown in Fig. 3.21.
- (b) **Participation of carbanion of TPP ( $-:^+TPP$ ) in the decarboxylation of pyruvic acid.** The thiazole carbanion participates in the nucleophilic attack on the ketocarbonyl of pyruvic acid to form the adduct (Fig. 3.22). The latter then suffers decarboxylation in the presence of the enzyme pyruvate decarboxylase

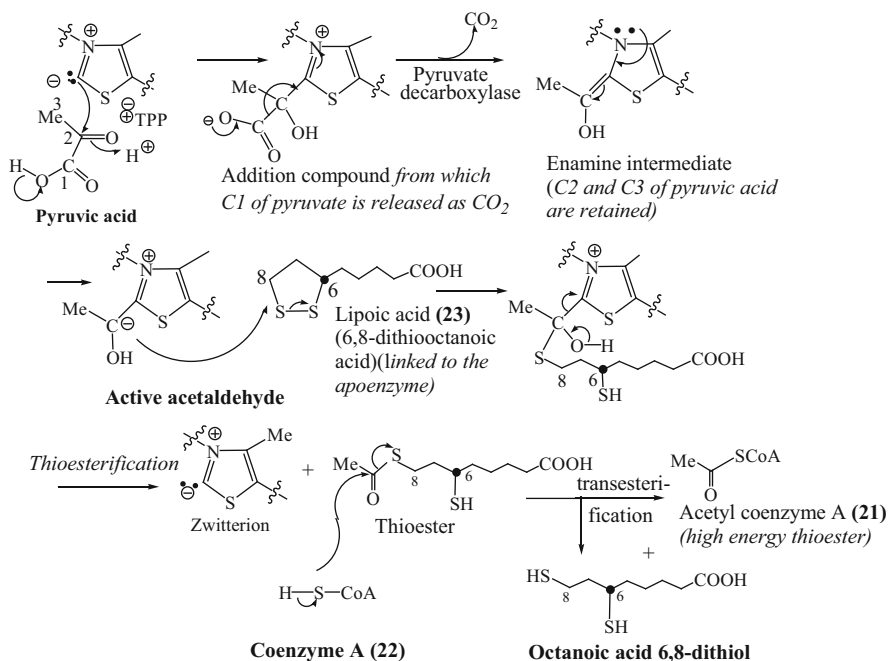
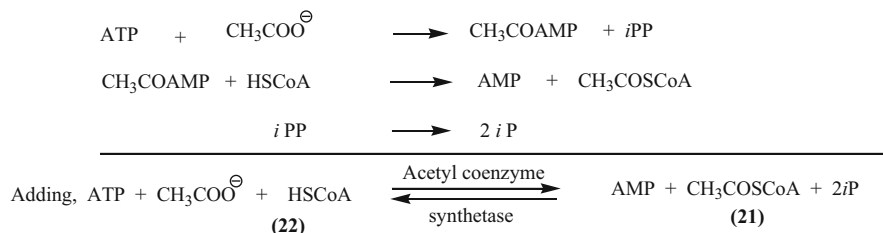


Fig. 3.22 Formation of acetyl coenzyme A from pyruvic acid



**Fig. 3.23** Formation of acetyl coenzyme A (21) from coenzyme A (22)

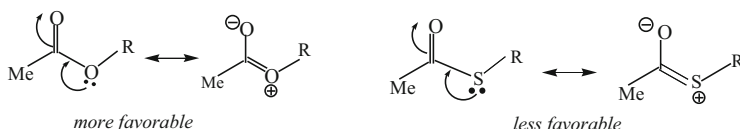
to form an **active acetaldehyde** via an enamine intermediate. The former attacks the disulfide bond of the liponic acid residue linked to the apoenzyme. The thioester thus formed by transesterification yields acetyl coenzyme A and octanoic acid 6,8-dithiol.

### 3.4.2 Formation of Acetyl Coenzyme A from Coenzyme A

Acetyl coenzyme A (21) is also formed by acetylation of coenzyme A (22) by acetate; the reaction is catalyzed by acetate thiokinase as shown in Fig. 3.23. The pyrophosphate (*i*PP) breaks down to inorganic phosphate (*i*P).

### 3.4.3 Functions of Acetyl Coenzyme

Acetyl coenzyme A (21) performs the pivotal role as the starter in the biosynthesis of molecules of different skeletal patterns. It is capable of transferring a C<sub>2</sub>-unit, like CH<sub>3</sub>CO or CH<sub>2</sub>CO moiety to appropriate substrates. It can undergo oligomerization via malonyl coenzyme A to give molecules with active ketomethylene groups, and it finds ways to enter into the *biosynthesis of polyketides, aromatic phenolic compounds and fatty acids* (Chap. 14). It is the key molecule of the several metabolic pathways like *mevalonic acid pathway* (Chap. 5) leading to many terpenoids and steroids and the citric acid cycle.



The reactivity of the thioester part of acetyl coenzyme A is due to two factors: (i) the thioester group is less stable than the ester group since the electron delocalization is more prominent in the latter; smaller volume of oxygen atom and its closer orbital energy than that of sulfur helps the overlapping of the lone pair more efficiently with the carbon orbitals, and hence the double bond character of C–S bond is less compared to the C–O bond in their respective esters. (ii) This makes the C–S bond weaker in addition to the more polarizability of the sulfur atom than oxygen; the thioester group is thus a better leaving group than the ester.

### 3.4.4 Enzymatic Conversion of Choline to Acetylcholine by Acetyl Coenzyme A

Acetylcholine (ACh) (25) and norepinephrine are important neurotransmitters which use different pharmacological receptors to mediate their end-organ responses. Acetylcholine is formed from choline (24) (Fig. 3.24) by the action of acetyl coenzyme A bound to the surface of the enzyme choline acetyltransferase (ChAT). The imidazole moiety of the enzyme promotes the removal of the alcoholic proton of choline (24) which is also bound to ChAT, generating a more nucleophilic center in choline, thus facilitates the acetyl group transfer and produces acetylcholine (ACh) (25) and coenzyme A (22).

**High energy transfer potential.** Acetyl coenzyme A is a small water-soluble high energy metabolite. It suffers hydrolysis, and the free energy change of the reaction is largely negative:



The reaction is thermodynamically favorable. The acetyl coenzyme A has a high acetyl transfer potential, the reaction being exergonic.

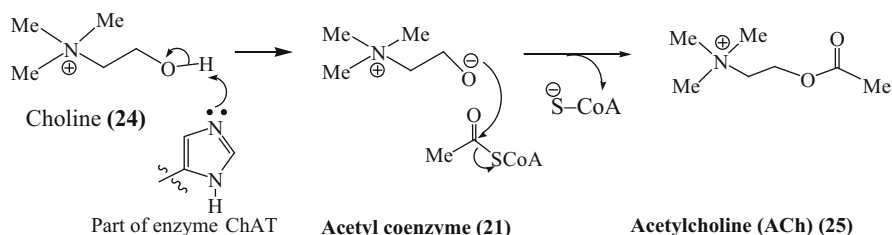


Fig. 3.24 Enzymatic conversion of choline to acetylcholine

### 3.5 Transamination, Isomerization, and Decarboxylation

Transamination is a very important biological event, a multistep reaction, catalyzed by enzymes called aminotransferases or transaminases. In a transamination reaction, the  $\alpha$ -amino group of an L-amino acid<sub>1</sub> is donated to the  $\alpha$ -carbon atom of an acceptor like an  $\alpha$ -keto acid<sub>2</sub>, *in a stereospecific manner*, leaving behind an  $\alpha$ -keto acid, the corresponding  $\alpha$ -keto acid analog of the amino acid<sub>1</sub>. The overall reaction and a specific example are shown in Fig. 3.25. In the transamination reactions, the removal of the  $\alpha$ -amino groups constitutes the first step in the catabolism of most of the amino acids. There is no net deamination in such reactions, e.g.,  $\alpha$ -ketoglutarate becomes aminated, while the  $\alpha$ -amino acid is deaminated. The transamination reaction of different L-amino acids with  $\alpha$ -ketoglutarate produces L-glutamate. The latter enters either into biosynthetic pathways or into a sequence of reactions producing nitrogenous waste products for excretion.

The aminotransferases are specific for a particular L-amino acid that donates the amino group and are named accordingly. The reactions catalyzed by the transaminases are completely reversible, having an equilibrium constant of nearly 1.0 ( $\Delta G^0 \approx 0$  kcal/mol).

The transamination is mediated by the most versatile of all coenzymes (or cofactors), pyridoxal-5'-phosphate (PLP), the vitamin form of which is the corresponding alcohol, pyridoxine (vitamin B<sub>6</sub>). The overall established mechanism of the PLP catalysis is delineated in two distinct halves in Figs. 3.26 and 3.27.

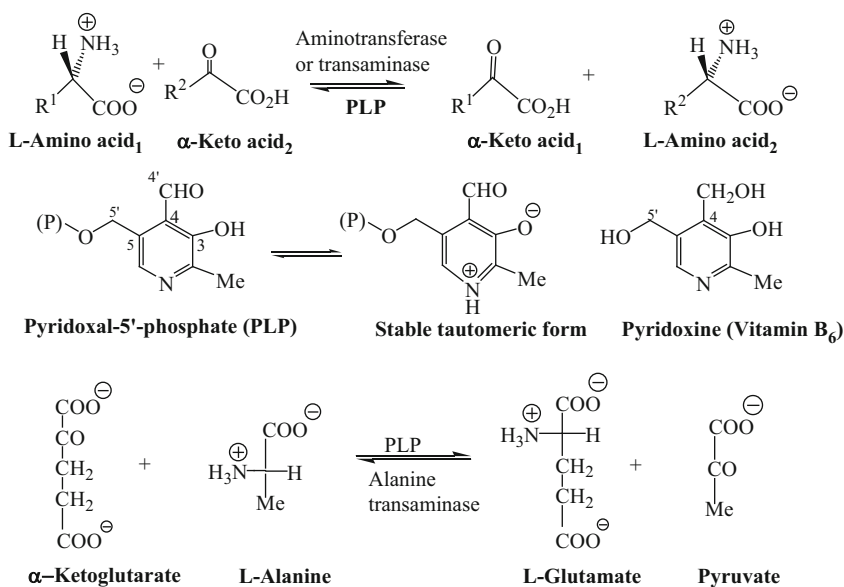
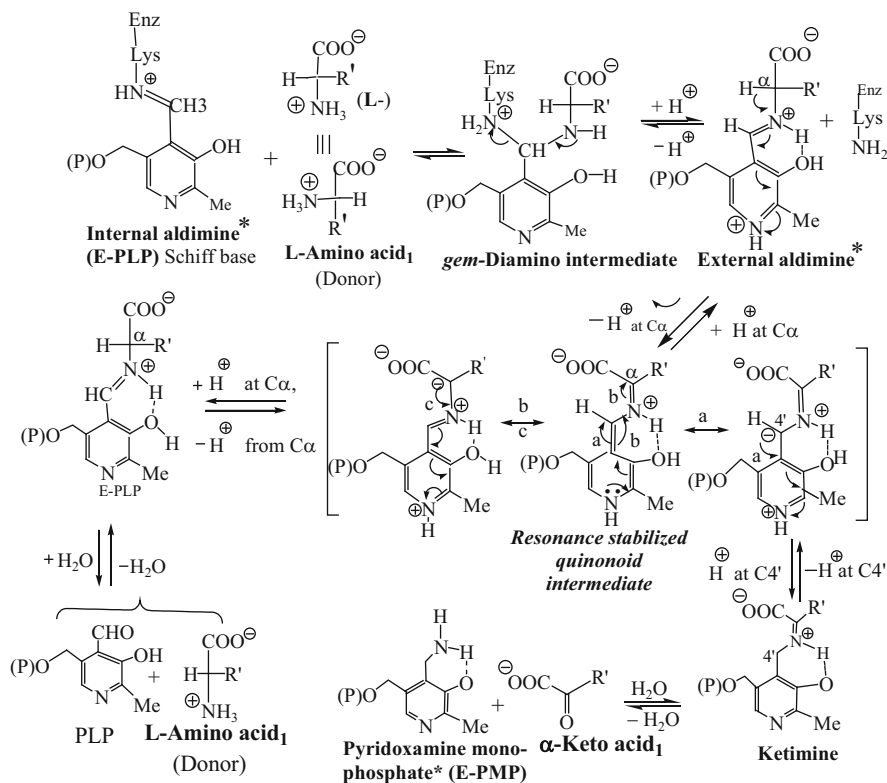


Fig. 3.25 Transamination (Aminotransferase reaction) :



\* *Tightly bound with the enzyme by multiple noncovalent interactions*

**Fig. 3.26** Mechanism of the first half of the PLP catalyzed transamination reaction

The cofactor PLP is initially bound through multiple noncovalent interactions, and also covalently with the active site of the PLP-dependent enzyme through an imine (Schiff base) linkage, and is commonly called *internal aldimine* or E-PLP, by reaction of 4-CHO of the PLP with the ε-amino group of a lysine residue of the enzyme. The E-PLP is then attacked by the α-amino group of the donor L-amino acid (substrate) to form a *gem*-diamine intermediate that rapidly collapses to a new Schiff base of the coenzyme–substrate complex. The new aldimine thus formed is referred to as the ‘*external aldimine*’. Loss of proton at the α-carbon (of the amino acid), aided by protonation of the pyridine nitrogen (acting as electron sink), gives rise to a resonance stabilized quinonoid intermediate. This species can be reprotonated through addition of H<sup>+</sup> at C4’. Hydrolysis, of the resulting ketimine gives pyridoxamine phosphate (PMP) and a new keto acid (as in the first half of the transamination reaction). Reprotonation of the quinonoid intermediate may also take place at the amino acid α-C to regenerate the catalyst PLP and the original amino acid (Fig. 3.26), through the reformation of E-PMP.

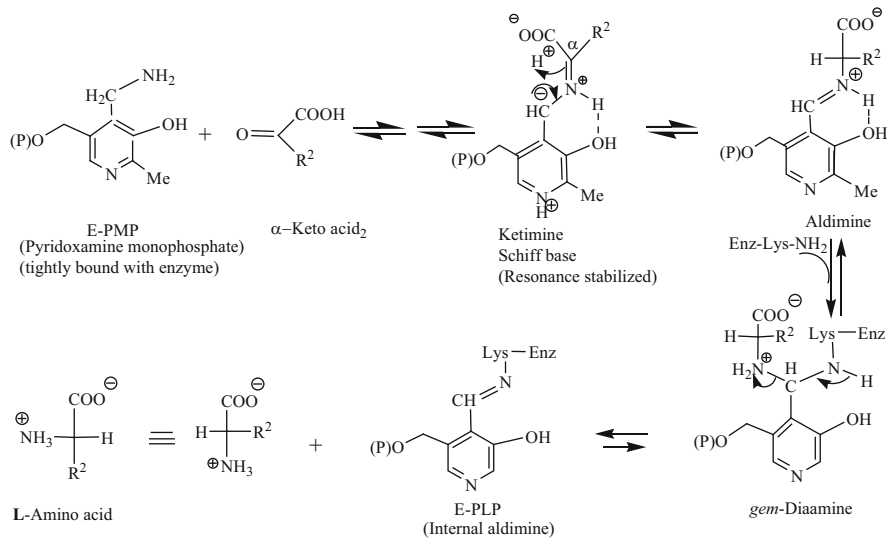


**Fig. 3.27** Mechanism of the second half of the PLP catalyzed transamination reaction

Thus the first half of the *transamination reaction* constitutes the following:

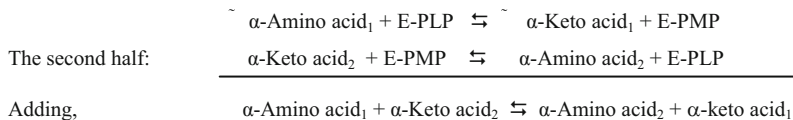


**Fig. 3.28** Transamination reaction

The second half of the transamination process, catalyzed by the specific amino-transferase is completed in a reversal of the preceding reaction pathway (Fig. 3.27). The second  $\alpha$ -keto acid which replaces the released one, condenses with the generated PMP (tightly bound with the enzyme and known as E-PMP) to form the corresponding ketimine Schiff base, deprotonation at C4'—the pyridine ring acting as the electron sink, leading to the formation of the resonance stabilized C $\alpha$  carbanion, followed by protonation to form an aldimine. The latter gives rise to a different L-amino acid, and regenerates E-PLP, through the intermediacy of a *gem*-diamine (Fig. 3.27). The E-PMP generated in the first half of the transamination is thus recycled to the E-PLP formed in the second half (Fig. 3.28).

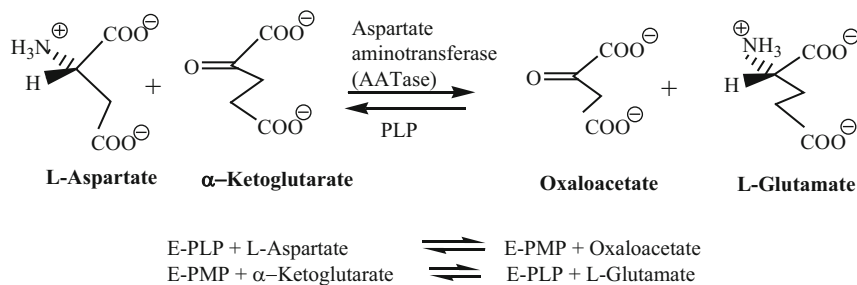


**Fig. 3.29** The most studied transamination reaction

### 3.5.1 Transamination by Aspartate Aminotransferase

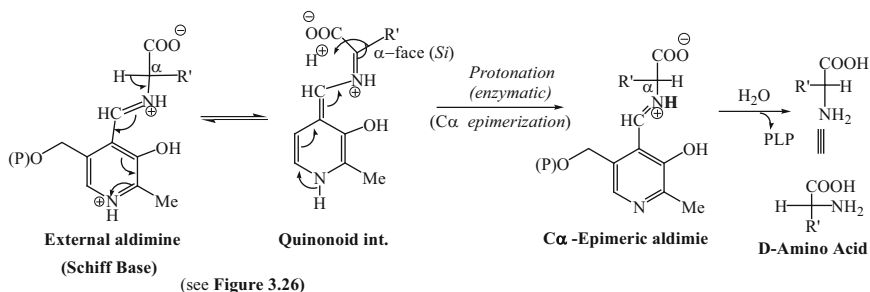
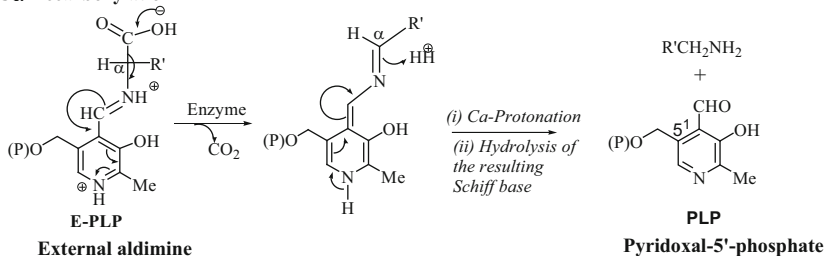
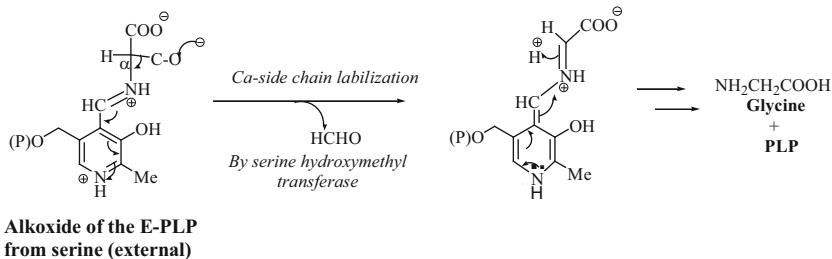
Aspartate aminotransferase (AATase) is *the most thoroughly studied* of all the PLP-dependent enzymes involved in amino acid metabolism. The reversible interconversion of L-aspartate and  $\alpha$ -ketoglutarate to oxaloacetate and L-glutamate is catalyzed by AATase (Fig. 3.29). The enzyme operates through a mechanism already discussed with two distinct half-reactions constituting a full catalytic cycle as illustrated in Fig. 3.29.

## 3.5.2 Some Interesting Concepts of The PLP-Catalyzed Transamination Reactions

### 3.5.2.1 Racemization and Decarboxylation

The external aldimine is a common intermediate in all PLP-dependent amino acid reactions. The pyridinium ring in the Schiff base (external aldimine) (Fig. 3.26), being electron deficient, can act as an electron sink and can trigger the breaking of all the four bonds to  $\text{C}\alpha$ , *i.e.*,  $\text{C}\alpha\text{-H}$  or  $\text{C}\alpha\text{-COOH}$  or  $\text{C}\alpha\text{-R}$  or  $\text{C}\alpha\text{-N}$ , being labilized by PLP-dependent enzymes. Abstraction of the  $\text{C}\alpha$  proton by an enzymatic base gives rise to the resonance stabilized  $\text{C}\alpha$  carbanion which may also undergo inversion and pick up a proton from the stereochemically opposite face to form the  $\text{C}\alpha$ -epimeric aldimine. The latter on hydrolysis gives rise to the corresponding D-amino acid (Fig. 3.30). The racemases thus provide D-amino acids for bacterial cell wall synthesis.

Breaking of the  $\text{C}\alpha\text{-COOH}$  bond effects decarboxylation and eventually leads to the formation of the amine  $\text{RCH}_2\text{NH}_2$  as outlined in Fig. 3.30. This type of reaction is physiologically very important for mammals. Decarboxylation of glutamic acid produces  $\gamma$ -aminobutyric acid (GABA), a major inhibitory neurotransmitter. Dopamine, the immediate precursor of the hormone epinephrine, is

**C $\alpha$ -epimerization****C $\alpha$ -Decarboxylation****C $\alpha$  Side chain replacement**

**Fig. 3.30** PLP-dependent amino acid C $\alpha$  epimerization (racemization), decarboxylation and C $\alpha$  replacement reactions via external aldimine)

formed by the decarboxylation of dihydroxyphenylalanine (DOPA). Likewise, histamine and serotonin, which have important complex biological functions, are formed by the decarboxylation of histidine and 5-hydroxytryptophan, respectively.

**3.5.2.2 C $\alpha$  Side Chain Replacement**

An example of such a reaction is that catalyzed by serine hydroxymethyl transferase (Fig. 3.30). Here, the replacement of the hydroxymethyl group by a proton is initiated by the formation of the serine alkoxide ion which collapses to formaldehyde, and the C $\alpha$  carbanion eventually gives glycine.

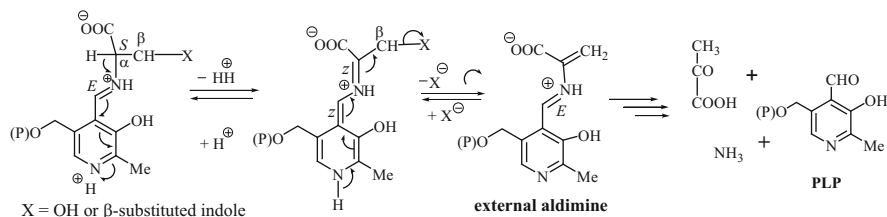


**Fig. 3.31**  $\beta$ -Elimination reactions catalyzed by PLP-dependent enzymes

### 3.5.2.3 PLP-Catalyzed Reaction at $\beta$ -Carbon Atom of Amino Acids

The catalytic power of PLP is observed in reactions involving groups on the  $\beta$ -carbon (Fig. 3.31). Specific enzyme catalyzed  $\beta$ -elimination takes place when a good leaving group is present. Serine dehydratase or tryptophanase is an example of an enzyme when serine or tryptophane is used. The  $\text{C}\alpha\text{-H}$  bond is just broken to give a delocalized carbanion, which subsequently expels the leaving group (here  $\text{H}_2\text{O}$ ; indole when tryptophan is used) to form the external aldimine. The latter is hydrolyzed to the free enamine which decomposes to pyruvic acid, ammonia, and PLP.

### 3.5.2.4 Stereochemical Concepts of the Pyridoxal Phosphate (PLP) Catalyzed Reactions

Much work has been done in this area and the salient interesting points are summarized below:

Reaction specificity imposed by the enzyme protein upon the system is achieved by control of the conformation around  $\text{C}\alpha\text{-N}$  bond of the substrate cofactor complex. The bond to be broken must be orthogonal to the plane of the conjugated  $\pi$  system. In this conformation, the breaking  $\sigma$ -bond achieves maximal orbital overlap with the  $\pi$  system, resulting in a substantial rate enhancement. Thus, the pyridine ring, the  $\text{C}4'$  amino nitrogen and  $\text{C}\alpha$  of the coenzyme-substrate complex must lie in a plane for resonance stabilization. Hence, the three conformers (A), (B), and (C) (Fig. 3.32) represent the orientations of the complex for the enzyme-catalyzed cleavage of the  $\text{C}\alpha\text{-H}$  bond, the  $\text{C}\alpha\text{-COOH}$  bond, and the  $\text{C}\alpha\text{-C}\beta$  bond, respectively.

The reactions of PLP enzymes take place on one face of the planar PLP-substrate complex—the *exposed* or *solvent* face is the *Si* face at  $\text{C}4'$  of the cofactor—the other face being covered by the protein. A chemically intuitive concept is that the enzyme binds the relatively rigid PLP cofactor at the points: pyridine N, and the phosphate, and the third point is probably the single distal carboxyl group on the substrate, resulting in a particular conformation by the  $\text{C}\alpha\text{-N}$  bond. It has been

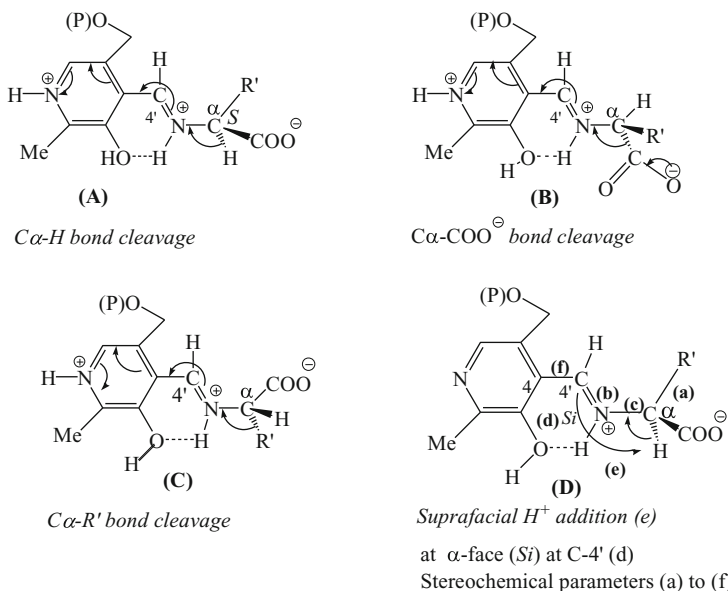
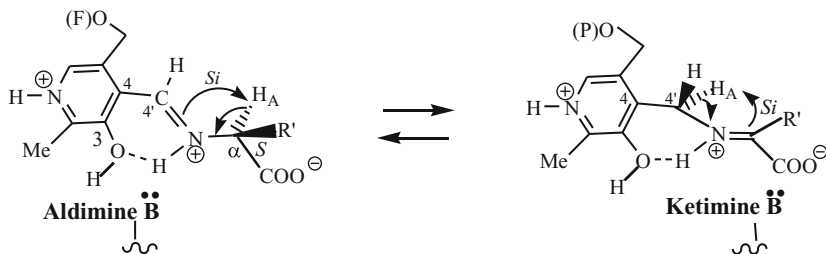


**Fig. 3.32** Optimal conformations about the  $C\alpha$ -N bond for cleavage of the  $C\alpha$ -H(A),  $C\alpha$ -COO<sup>⊖</sup>(B), or  $C\alpha$ -R'(C) bonds of L-amino acid, and suprafacial H<sup>+</sup> addition. Stereochemical parameters of enzymatic transformation (D)

shown that group interchanges take place *in a retention* mode and proton transfer with *suprafacial* geometry.

The stereochemistry of the whole transamination reaction, catalyzed by the given specific enzymes and the cofactor PLP, thus involves the following six parameters [(D), Fig. 3.32] established through experiments of many workers.

- Configuration at  $C\alpha$  of the substrate:** Only the L-enantiomer (and not D-) of an  $\alpha$ -amino acid reacts.
- Configuration of the  $C4' = N$  double bond** must be *E* (or *trans*): a *Z* (or *cis*) double bond will not be coplanar with the pyridine ring due to steric interference by the adjacent ring substituents (*ortho*).
- Conformation around the  $C\alpha$ -N bond.** As discussed earlier, the bond to the  $C\alpha$  to be broken must be perpendicular to the plane of the conjugated  $\pi$  system [as shown in conformers (A), (B), and (C) in Fig. 3.32].
- Site of proton addition or deprotonation at  $C4'$**  has been shown to be on the *Si* face or  $\alpha$ -face of the structure (D) of the coenzyme-substrate or the coenzyme-intermediate complex, as revealed from studies with many specific transaminases.
- Mode of prototropic shift from  $C\alpha$  of the substrate to  $C4'$  of PLP** has been demonstrated to be *suprafacial* (not *antarafacial*) by experiments involving internal transfer of tritium and deuterium. Internal proton transfer in aldimine



**Note:** Protonation of pyridine N makes the  $\alpha$ -H<sub>A</sub> / 4' H<sub>A</sub> more acidic.

**Fig. 3.33** Aldimine ketimine tautomerization in the transamination of an L-amino acid

ketimine tautomerization (Fig. 3.33) strongly suggests that the deprotonation and protonation are mediated by the simple base which necessitates *suprafacial* nature of the process. Thus, for such reaction the conformation around C $\alpha$ -N single bond must be such that C $\alpha$ -H is exposed on the side of the complex corresponding to the *Si* face at C4', *i.e.*, in an L-amino acid-coenzyme complex the carboxyl group and C4' would be *trans* to each other (Fig.3.33).

- (f) **Conformation around C4-C4' bond.** Model studies and calculations show that in the absence of the enzyme, pyridoxal Schiff bases prefer a *cisoid* conformation (C4' = N imine bond is on the same side of C4-C4' bond as the C3-OH). Of course, during catalytic process a reorientation of the cofactor takes place. X-ray diffraction studies revealed that the cofactor-lysine Schiff base is in the *cisoid* conformation with the C4' = N roughly coplanar with the pyridine ring, and the *Si* face against a  $\beta$ -sheet of the protein. Moreover, the *cisoid* form of all aldimines and ketimines are expected to be more stabilized than the *transoid* form, by H-bonding between oxygen of OH and 4'-NH, as shown in the conformers (A) to (D).

## 3.6 Addition of C<sub>1</sub>-Unit with AdoMet (SAM)

### 3.6.1 Methylation

In the biosynthetic process of C<sub>1</sub>-unit addition, the enzymatic transfer of a methyl group takes place from L-methionine. The latter, prior to its participation in methyl transfer, is activated by its conversion to S-adenosylmethionine (SAM or AdoMet) by an unusual S<sub>N</sub>2 reaction with ATP by the action of methionine adenosyl transferase, in which the nucleophilic sulfur atom of methionine attacks the C5' on the ribose unit expelling the inorganic triphosphate (*i*PPP) rather than attacking any phosphorus atom. Thus, an unstable *sulfonium ion* is formed having a

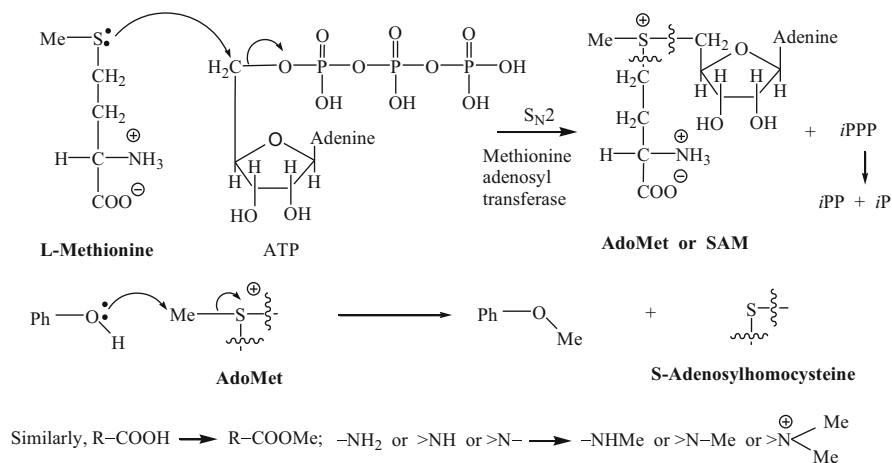


**Fig. 3.34** Biogenetic O-methylation or N-methylation by the strong electrophile *S*-adenosylmethionine (SAM or AdoMet)

high thermodynamic tendency to transfer its methyl group and gets neutralized. The expelled triphosphate is enzymatically hydrolyzed to pyrophosphate (*i*PP) and orthophosphate (*i*P) (Fig. 3.34). SAM is a potent strong methylating agent and it undergoes facile attack by oxygen or nitrogen nucleophiles.

### 3.6.2 Formation of Methylenedioxy Bridge and Its Reductive Opening [8, 9]

The methylenedioxy moiety is formed via regiospecific monomethylation of an *ortho*-dihydroxybenzene system, followed by the removal of a hydride (*cf.* anti elimination of e<sup>-</sup> and H<sup>+</sup>) to form a carbocation, stabilized by resonance by a nonbonding lone pair of the adjacent oxygen (see Fig. 3.35). The *ortho* OH then attacks the carbocation center to form a methylenedioxy bridge, a common functional moiety in many natural products.

Studies with labeled AdoMet showed the stereochemical implication of the transformation of a labeled methoxy into a labeled methylenedioxy group, followed by reductive opening of the latter to a labeled methoxy function, as illustrated in the biosynthesis of *protoberberine type* isoquinoline alkaloids by enzymes from plant cell cultures, *e.g.*, conversion of 2-O-demethyljatrorrhizine (**1**) to labeled *jatrorrhizine* (**4**) via (**2**) and labeled *berberine* (**3**) (Fig. 3.35).

The reaction sequence involves the transfer of a chiral methyl group from SAM to oxygen of a protoberberine alkaloid (**1**) to form (**2**) with inversion of configuration. The latter is then fed into callus cultures of *Berberis koetianeana*, which

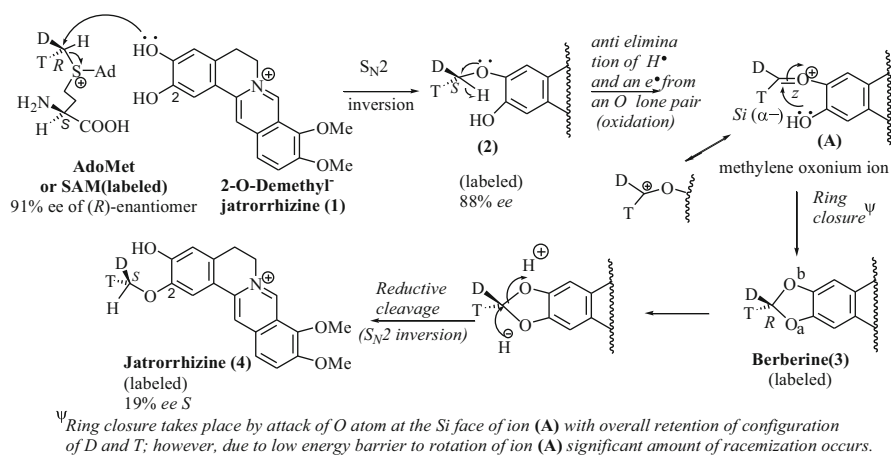


**Fig. 3.35** Formation of the methylenedioxy bridge of berberine and its subsequent reductive opening to form the hydroxy/methoxy functions of jatrorrhizine with stereochemical mechanism.

converted it via berberine (3) into jatrorrhizine (4). By degradation, it was found that the chiral methyl groups in the protoberberine (2) and jatrorrhizine were both having (*S*) configuration.

It follows that probably the oxidative closure to form the methylenedioxy bridge occurs with retention of configuration, and the labeled methylenedioxy bridge reductively opens up with inversion of configuration. Thus, the migration of the chiral methyl from the original oxygen to the adjacent (vicinal) oxygen is formally equivalent to inversion. The methyleneoxonium ion (A) has a significantly lower energy barrier to rotation, and can to a significant extent undergo configurational isomerization prior to attack of oxygen on the methylene carbon, accounting for partial racemization.

### 3.6.3 *N*-Methylation and Formation of a Methylene Bridge Between Nitrogen and Carbon [10]

The conversion of  $>NH$  to  $-NCH_3$  by transfer of the chiral methyl from labeled Ado-Met to the nitrogen proceeds clearly with complete inversion of configuration. The subsequent transformation of the chiral *N*-methyl group into a chiral methylene bridge between nitrogen and carbon takes place in presence of the specific enzyme. This sequence of reactions has been demonstrated to lead to labeled scoulerine, a tetrahydroprotoberberine type alkaloid, as shown in Fig. 3.36.

From the tritium NMR analysis of scoulerine formed, it is apparent that the replacement of a hydrogen of the chiral *N*-methyl group by the aromatic ring carbon

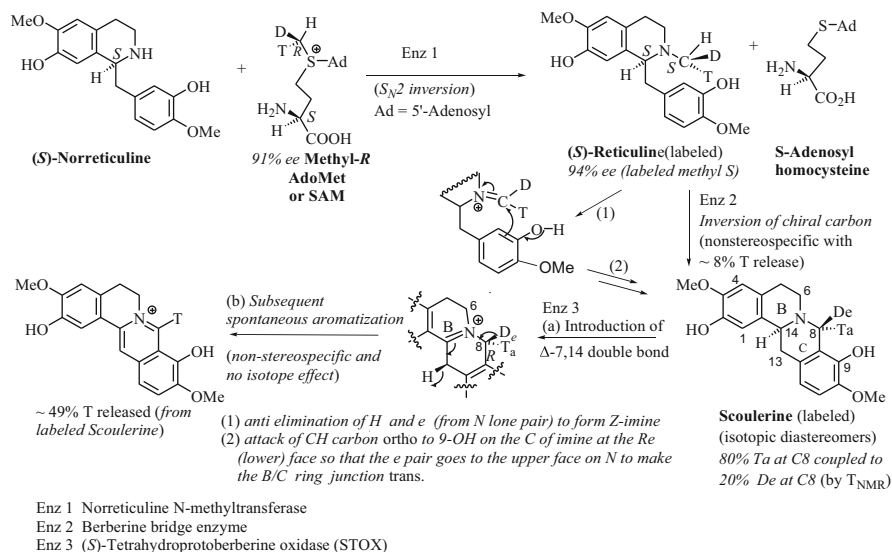


**Fig. 3.36** Enzymatic reaction sequence in the N-methylation of norreticuline, and generation of the berberine bridge followed by its further oxidation

has occurred *with inversion*, and that the hydrogen abstraction has an isotope effect  $k_{\text{H}}/k_{\text{D}}$  4. It is observed that in the berberine bridge the enzyme releases about 8 % T from (S)-Me group of (S)-reticuline, consistent with the observed isotope effect of 4. Subsequent addition of the enzyme STOX leads to 49 % T release, nearly half of the remaining T from the two *isotopically diastereomeric* substrates indicating *non-stereospecific nature of the reaction* lacking any isotope effect. Thus it is postulated that STOX only catalyzes the introduction of a  $\Delta^{7,14}$  double bond, and subsequent aromatization occurs spontaneously (Fig. 3.36).

## 3.7 C- and O-Alkylation

### 3.7.1 C and O-Alkylation of Phenols

Both C- and O-alkylation of phenols are quite prevalent in natural products. The alkyl groups mostly consist of methyl and prenyl groups. SAM (AdoMet) serves as the methylating agent (Sect. 3.6), and various prenyl groups as their pyrophosphates act as the prenylating agents. Figure 3.37 depicts different types of probable C- and O-prenylation and cyclization of polyphenolic compounds like resorcinol.

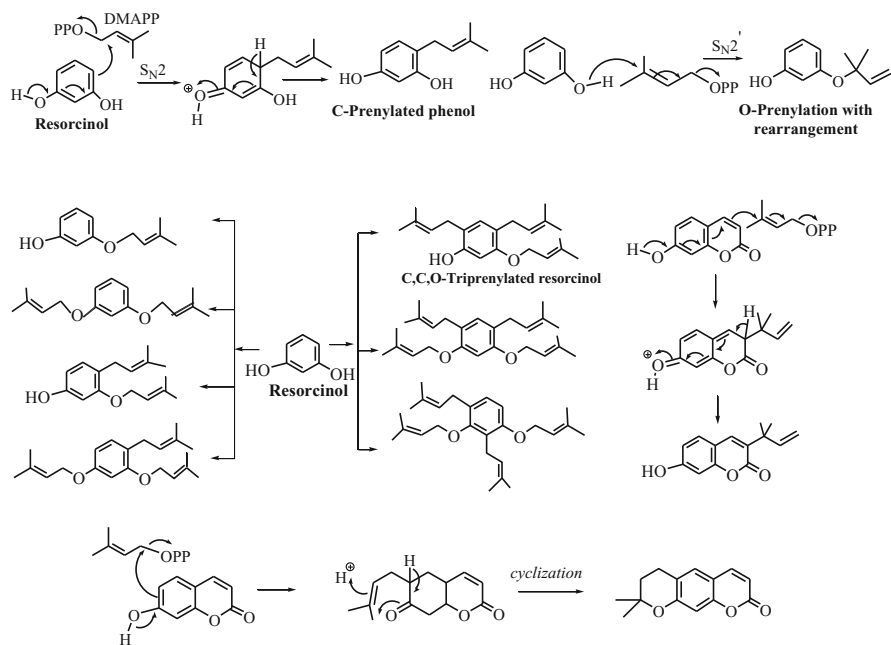


**Fig. 3.37** Different types of probable C- and O-prenylations of polyphenols like resorcinol, and cyclization

The formation of  $C_5$ ,  $C_{10}$ ,  $C_{15}$ , and  $C_{20}$  prenyl pyrophosphates has been discussed in detail in Chap. 5. Of all the prenyls,  $C_5$  and its modified forms occur most prevalently. Since the leaving groups of the natural alkylating agents do not vary, their influence on the proportion of the C- and O-alkylation, as observed in the laboratory reactions with different leaving groups, does not occur. Further, the specificity of the catalytic enzymes also plays an important role in the *regiospecificity* of alkylation, as is observed in coumarins, xanthenes, flavones, etc. Coumarins provide best examples of such specificity. Figure 3.38 displays some examples of regiospecific methylation, C- and/or O-prenylation/s, prenyl chain modification of *resorcinol*, *umbelliferone*, and *6-hydroxyumbelliferone* to produce natural coumarins [11]. Sometimes prenyl groups are locked in a cyclic moiety (e.g., *pyranocoumarin* or *furanocoumarin* derivatives). In coumarins, perhaps the largest number of biogenetic modifications of the simple isoprene unit occurs, and also quite often they appear in a cyclic form [8]. C-Alkylation takes place at the available *ortho*- position of an activating group like OH before it may undergo O-alkylation [11].

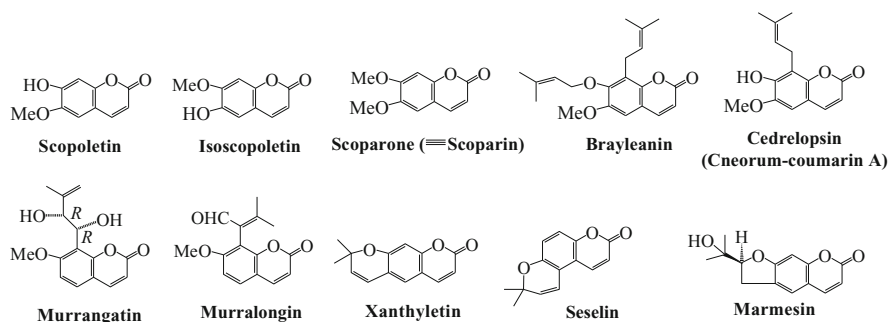


**Fig. 3.38** Regiospecific methylation, C- and O- prenylation, prenyl chain modification, cyclization etc. to form some natural coumarins

### 3.7.2 C-Methylation and Modification of Cycloartenol Side Chain to Form Phytosterols [12, 13]

All phytosterols except cholesterol contain extra carbon atom/s at C24 of the side chain compared to its precursor cycloartenol. Cholesterol occurs mainly in the animal organisms and less abundantly in plant cells. Cycloartenol is metabolized in the plant cells to yield phytosterols including cholesterol (Chap. 11). The presence of a double bond ( $\Delta^{24}$ ) in the side chain of the precursor plays a vital role as an obligatory  $\pi$ -bond nucleophile towards the electrophilic SAM (AdoMet). The electrophilic addition of the methyl group takes place from the *Si* ( $\alpha$ -) face of the double bond at C24. Through labeling experiments it has been shown that the resulting C25 carbocation **A** is quenched by delivery of hydride either from NADPH at the *Si* ( $\alpha$ -) face of the cation to form **campesterol**, or from the adjacent C23 methylene at the appropriate *Re* face, followed by loss of  $H^+$  from C22 to form **ergosterol** having (24*R*) and *E* stereochemistry of the 22–23 double bond (Fig. 3.39). The newly formed  $sp^3$  chiral carbon always appears in one epimeric form—a characteristic of enzymatic reaction. The carbocation **A** may also be quenched to a double bond by loss of  $H^+$  from the methyl group, followed by methylation by SAM to form the cation **B**, which upon delivery of hydride by NADPH at the *Si* ( $\alpha$ -) face of the cation forms **sitosterol**. Alternatively, the cation **B** may be quenched by a hydride shifted from C23 giving rise to the C23 cation, followed by loss of the appropriate proton to form **stigmasterol** having (24*S*) and *E* stereochemistry of the 22–23 double bond. Thus, in cases of ethyl group ( $C_2$ ) containing sterols (sitosterol and stigmasterol) two methylations by SAM take place (Fig. 3.39).

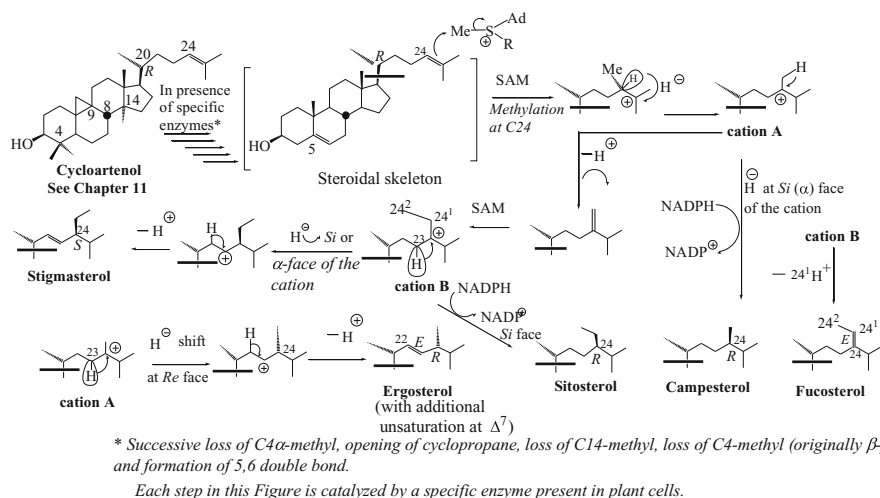


**Fig. 3.39** Side chain methylation and modifications to form different phytosterols

### 3.8 Other Important Biological Events

Many reactions/rearrangements like Wagner–Meerwein rearrangement, Baeyer–Villiger oxidation, Michael addition, Markovnikov addition, less likely anti-Markovnikov addition, diradical coupling reactions, etc., and rarely 3,3-sigmatropic rearrangement do occur in plant cells, being catalyzed by suitable enzymes during the biosynthesis of natural products with various skeletal patterns. These have been discussed in the biosyntheses of pertinent natural products in different chapters.

## References

1. Bill Bryson, *A Short History of Nearly Everything*, Black Swan, **2004**, p.362.
2. G. Feher, Identification and Characterization of the Primary Donor in Bacterial Photosynthesis: A Chronological Account of an EPR/ENDOR Investigation (The Bruker Lecture), *J. Chem. Soc. Perkin Trans. 2*, **1992**, 1861-1874.
3. M. B. Bishop and C. B. Bishop, Photosynthesis and Carbon Dioxide Fixation, *J. Chem. Educ.*, **1987**, *64*, 302-305.
4. R. Sterner and B. Höker, Catalytic Versatility, Stability and Evolution of the (β<sub>α</sub>)<sub>8</sub>-Barrel Enzyme Fold, *Chem. Rev.*, **2005**, *105*, 4038-4055.
5. M. D. Hatch and C. R. Slack, Photosynthesis by Sugarcane Leaves. A New Carboxylation Reaction and the Pathway of Sugar Formation, *Biochem. J.*, **1966**, *101*, 103-111.
6. M. D. Hatch, C<sub>4</sub>-Photosynthesis. An Unlikely Process Full of Surprises, *Plant Cell Physiology*, **1992**, *33*, 332-342.

7. Ronald Breslow, On the Mechanism of Thiamine Action. IV. Evidence from Studies on Model Systems, *J Am Chem Soc.*, **1958**, *80*, 3719-3726.
8. Heinz G. Floss, Thomas Frenzel, David R. Houck, Lai-Duien Yuen, Pei Zhou, Lynne D. Zydowsky, and John M. Beale, Stereochemistry of One-carbon Metabolism in Aerobes and Anaerobes, in *Molecular Mechanisms in Bioorganic Processes*, Ed. C. Bleasdale and B. T. Goldberg, Royal Society of Chemistry, **1990**, pertinent pages 31-37, and relevant references cited.
9. Motomasa Kobayashi, Thomas Frenzel, Jonathan P. Lee, Meinhart H. Zenk, and Heinz G. Floss, Stereochemical Fate of O-Methyl Groups in the Biosynthesis of Protoberberine Alkaloids, *J. Am. Chem. Soc.*, **1987**, *109*, 6184-6185.
10. Thomas Frenzel, John M. Beale, Motomasa Kobayashi, Meinhart H. Zenk, and Heinz G. Floss, Stereochemistry of Enzymatic Formation of the Berberine Bridge in Protoberberine Alkaloids, *J. Am. Chem. Soc.*, **1988**, *110*, 7878-7880.
11. R. D. H. Murray, Naturally Occurring Plant Coumarins, *Fortschr. Chem. Org. Naturstoffe*, **1997**, *72*; **1991**, *58*; **1991**, *35*; **1997**, *72* **2002**, *83*
12. Geoffrey D. Brown, The Biosynthesis of Steroids and Terpenoids, *Nat. Prod. Rep.*, **1998**, 653-696.
13. H. H. Rees and T. W. Goodwin, Biosynthesis of Terpenes, Steroids and Carotenoids in *Biosynthesis*, Volume 1, *Specialist Periodical Reports*, The Chemical Society, London, **1972**, pp. 59-118, pertinent pp. 93-99.

### ***Further Reading***

- P. Suppan, *Principles of Photochemistry* (Monograph for Teachers), The Chemical Society, London, **1973**, pp. 59-62.
- T.A. Geissman and D.H.G. Crout, *Organic Chemistry of Secondary Plant Metabolism*, Freeman, Cooper & Company, San Francisco, **1969**.
- A. Cox and T.J. Kemp, *Introductory Photochemistry*, McGraw-Hills Book Company (UK) Limited, England, **1971**, pertinent pages 166-171.
- Jeremy M. Berg, John L. Tymoczko and Lubert Stryer, *Biochemistry*, 6th Edition, Chapter 20, W.H. Freeman & Company, New York, **2007**.
- Hans-Walter Heldt, *Plant Biochemistry*, Academic Press (An Imprint of Elsevier), **2005** (3rd edn.), pp.45-66, 165-192, 213-242.
- Albert L. Lehninger, David L. Nelson and Michael M. Cox, *Principles of Biochemistry*, 2nd Edn., Worth Publishers, New York, **1992**.
- Christopher K. Mathews, K.E. van Holde and Kevin G. Ahern, *Biochemistry*, 3rd Edn., An Imprint of Addition Wesley Longman Inc., San Francisco, New York, **2000**.
- Robert Ruffolo Jr., Physiology and Biochemistry of the Peripheral Nervous System, Chapter 8 in *Human Pharmacology* (Molecular to Clinical), Editors, Theodora M. Brody, Joseph Larner, Kenneth P. Minneman and Harold C. Neu, Mosby, St. Louis, 2nd Edn., **1995**.



<http://www.springer.com/978-3-642-45409-7>

Chemistry of Plant Natural Products  
Stereochemistry, Conformation, Synthesis, Biology, and  
Medicine

Talapatra, S.K.; Talapatra, B.

2015, LXIII, 1180 p. 1015 illus., 21 illus. in color. In 2  
volumes, not available separately., Hardcover

ISBN: 978-3-642-45409-7